

SEISMIC RISK STUDIES, WESTERN GULF OF ALASKA

by

Hans Pulpan and Juergen Kienle

**Geophysical Institute
University of Alaska**

Final Report
Outer Continental Shelf Environmental Assessment Program
Research Unit 251

August 1984

TABLE OF CONTENTS

	List of Figures	373
	List of Tables	375
	Acknowledgements	377
I.	SUMMARY	378
II.	INTRODUCTION	379
III.	SOURCES , METHODS, AND RATIONALE OF DATA COLLECTION	380
	High-Gain Seismic Network	380
	Strong-Motion Instruments	387
IV.	RESULTS AND DISCUSSION	388
	Seismicity and Seismic Source Zone*	388
	Shallow Thrust Zone	388
	Faults	393
	Earthquake Activity of the Kodiak Shelf	395
	Intermediate Depth Earthquake Activity	405
	Seismic Exposure Studies	415
V.	CONCLUSIONS	415
VI.	REFERENCES	418
	APPENDIX: EPICENTER PLOTS FOR 1978-1982	423

LIST OF FIGURES

- Figure 1. Aftershock zones of great earthquakes and location of seismic gaps of the Aleutian-Alaska arc system. The arrows indicate the convergence direction between the Pacific and North American plates (after Sykes et al., 1981),
- Figure 2. Layout of the high-gain seismic network as it was operated through most of the study period.
- Figure 3. Typical technical layout of part of the high-gain seismic network.
- Figure 4. Typical system response of University of Alaska stations.
- Figure 5. Plate interaction in Alaska. Motion vectors of St. Elias, Yakutat and Wrangell blocks relative to North America after Lahr and Plafker (1980).
- Figure 6. Epicenters, volcanoes, depth contours to top of Benioff zone (50, 100, 150 km), and location of projection values for cross-sections shown in Figure 7. Epicenters from local network data July 1977 to June 1981.
- Figure 7. Cross-sectional views of Benioff zone along lines A-A', B-B', C-C' shown in Figure 6. No vertical exaggeration. Land masses (solid black), the position of the trench, and location of volcanoes are also shown. Shallow thrust zone is added schematically. Dashed lines show possible position of second seismic zone.
- Figure 8. Fault map of the Cook Inlet area (after Beikman, 1980).
- Figure 9. Depth distribution of selected events of Figure 11 for which depth phases could be well discerned on seismograms. Points A and B as in Figure 11. The numbers refer to Table 1. Events 35 and 36 were not part of the set of events which were relocated by the joint hypocenter determination (JHD) method.
- Figure 10. **Depth** distribution of **ISC** locations shown in **Figure 11**. **ISC** depths are based on reported depth phases. **Points A** and **B** as in Figure 10.
- Figure 11. **ISC** location of 34 earthquakes that were relocated by the JHD method.
- Figure 12. Location of the 34 events of Figure 11 after relocation.
- Figure 13. Epicenters of earthquakes relocated by the JHD method using regional network data.
- Figure 14. Cross-section of seismic events mapped in Figure 13.

- Figure 15. First motion fault plane solutions of **Benioff** zone events in Lower Cook Inlet.
- Figure 16. First motions (open circles for dilations, **full** circles for compression) of one of the events situated below the main **Benioff** zone in Lower Cook Inlet.

LIST OF APPENDIX FIGURES

- Figure A1. Epicenters of all earthquakes located during January-March, 1978. Symbols indicate depth range of events.
- Figure A2. Epicenters of all earthquakes located during April-June, 1978. Symbols as in Figure A1.
- Figure A3. Epicenters of all earthquakes located during July-September, 1978. Symbols as in Figure A1.
- Figure A4. Epicenters of all earthquakes located during October-December, 1978. Symbols as in Figure A1.
- Figure A5. Epicenters of all earthquakes located during 1979. Symbols as in Figure A1.
- Figure A6. Epicenters of all earthquakes located during January-June, 1980. Symbols as in Figure A1.
- Figure A7. Epicenters of all earthquakes located during July-December, 1980. Symbols as in Figure A1.
- Figure A8. Epicenters of all earthquakes located during January-June, 1981. Symbols as in Figure A1.
- Figure A9. Epicenters of all earthquakes located during July-December, 1981. Symbols as in Figure A1.
- Figure A10. Epicenters of all earthquakes located during 1982. Symbols as in Figure A1.

LIST OF TABLES

- Table 1. Locations determined by the JHD method of 34 events off Kodiak 1s1 and, In addition, the table provides the location of two events (#35 and #36) for which reliable depth phases could be identified on seismograms recorded at **WWSSN** stations.
- Table 2. Date and locations of events for which the first motion fault plane solutions shown in Figure 14 were obtained.
- Table 3. Nodal plane parameters for events of Table 2.
- Table 4. Stress axes parameters for the events of Table 2.

ACKNOWLEDGEMENTS

The program was funded by the National Oceanic and Atmospheric Administration's (NOAA) Outer Continental Shelf Environmental Assessment program (OCSEAP).

We would like to thank our program manager in Boulder, Joe Kravitz, and our program monitors in the Juneau OCSEAP Office, Rod **Combellik** and Laurie **Jarvela**, for their help and understanding during the course of this project.

Our thanks go also to George Lapiene and Mike Albertson of the Juneau Office for organizing helicopter, ship and other logistic support in the course of installing and maintaining the seismic station network. We also are indebted to the crews of the NOAA helicopters.

We owe special thanks to the management and flight crews of the U.S. Coast Guard flight station in Kodiak for valuable logistic support.

Technical work was performed by Steve Estes, Jim **Benich**, Ron Foster, Dick Abel, John Benevento and Jim Perry.

Data reduction and analysis were done by Dianne Marshall, Kathryn Engel, Bud Meyers and Hara **Biesiot**.

The program received substantial help from a concurrent one, funded by the U.S. Department of Energy (Contract No. **EY-76-S-06-2229**). A large portion of the seismic network was installed originally under that program. We are grateful for this support.

I. SUMMARY

This report summarizes the seismic hazard studies performed by us under the **OCSEA** program in the Semidi Island to Lower Cook Inlet section of the Alaska-Aleutian arc system. Central to our work was the collection of seismic data **by** operating a network of short-period seismograph stations in the above area. These data now permit the delineation and characterization of the seismic source zones of the area within the framework of plate tectonics. We also discuss a number of complimentary studies investigating or attempting to improve the resolution of the source zones: analysis of the location capability of the landbased network on the continental shelf area by analyzing the data obtained from the short term deployment of an array of ocean bottom seismometers on the shelf; relocation of hypocenters near Kodiak Island and Cook Inlet by the Joint Hypocenter Determination method; relocation of **teleseismically** recorded earthquakes in the Kodiak shelf section.

Attempts were made to collect strong ground motion data by deploying strong motion instruments at various sites during the study, but no useful records were recovered.

The contribution of this study lies in the description and characterization of the seismic source zones, thus providing important data for seismic exposure calculations. However, exposure calculations such as those performed under OSCEAP are presently limited by the rather large uncertainties associated with the **occurrence** times of great earthquakes along the arc system and the uncertainties in predicting strong ground motion at a particular site. Strong ground motion records and the study **of** the nature and mechanics of the shallow thrust **zone** seem to be the most important research topics for improving this situation.

II. INTRODUCTION

This study attempted to develop the scientific and technical basis for assessing the hazards associated with petroleum related developments on a portion of the Alaska Outer Continental Shelf which is subject to a very high level of seismic and volcanic activity. In many respects the Alaskan shelf is unique among the United States Outer Continental Shelf areas. The study was a data gathering program in its attempt to obtain data, pertinent to the seismic hazard problem, from a large and remote area at a resolution not previously available. It was a scientific program in its attempt to develop a better understanding of the fundamental processes underlying the seismic and volcanic activity, and it was an applied technical program in its attempt to quantify the associated risk. It was one of several such programs that covered a **1500 km** long portion of the eastern Aleutian-Alaska arc system. The easternmost and westernmost portions of the area have been identified as seismic gaps (the Yakataga and **Shumagin** seismic gaps, respectively) and are separated by the rupture zones of the 1964 ($M_w = 9.2$) earthquakes. Our own work concentrated on the section from the **Semidi** Islands to Lower Cook Inlet, encompassing a **large** portion of the 1964 rupture zone (Figure 1).

The ultimate purpose of a seismic risk analysis is to provide quantitative information about the seismic exposure a potential structure will be subjected to during its projected lifetime. This in turn requires information about (1) the location and configuration of seismic source zones, (2) the frequency of occurrence and magnitude distribution of earthquakes associated with individual source zones, (3) **the** nature of the motion generated at the earthquake source, (4) the modification of

that source motion as it propagates toward a particular site, and (5) the response of the structure to that input motion.

The program's principal contributions are associated with points (1) and (2), and to a more limited extent with (3). **Though** attempts were made to also contribute to (4) we were not successful in that **task**. The most important information with respect to (3) and (4) derives from strong motion recordings, still extremely limited in the various Alaskan **seismotectonic** environments. It is the lack of a sufficient number of such recordings in subduction zone environments that limits our understanding of the details of the earthquake rupture process and the attenuation of the strong ground motion with distance from the source. The meaningfulness of seismic hazards exposure calculations, such as were conducted in the course of OCSEAP, is therefore greatly limited. These problems have not been resolved satisfactorily in the course of the study.

The modification of strong ground motion by **surficial** geologic conditions (part of (4) above) is a site-specific problem and was not addressed at all in the program. Neither was the problem of the response of structures to strong earthquake ground motion.

III. SOURCES, METHODS AND RATIONALE OF DATA COLLECTION

High Gain Seismic Network

A short period, high gain seismic network was operated under this program. Earthquake **hypocentral** parameters were derived from the network data and assembled in the form of earthquake catalogs. These catalogs form the basis for identifying and delineating seismic source zones as well as for determining the associated magnitude-frequency relationships.

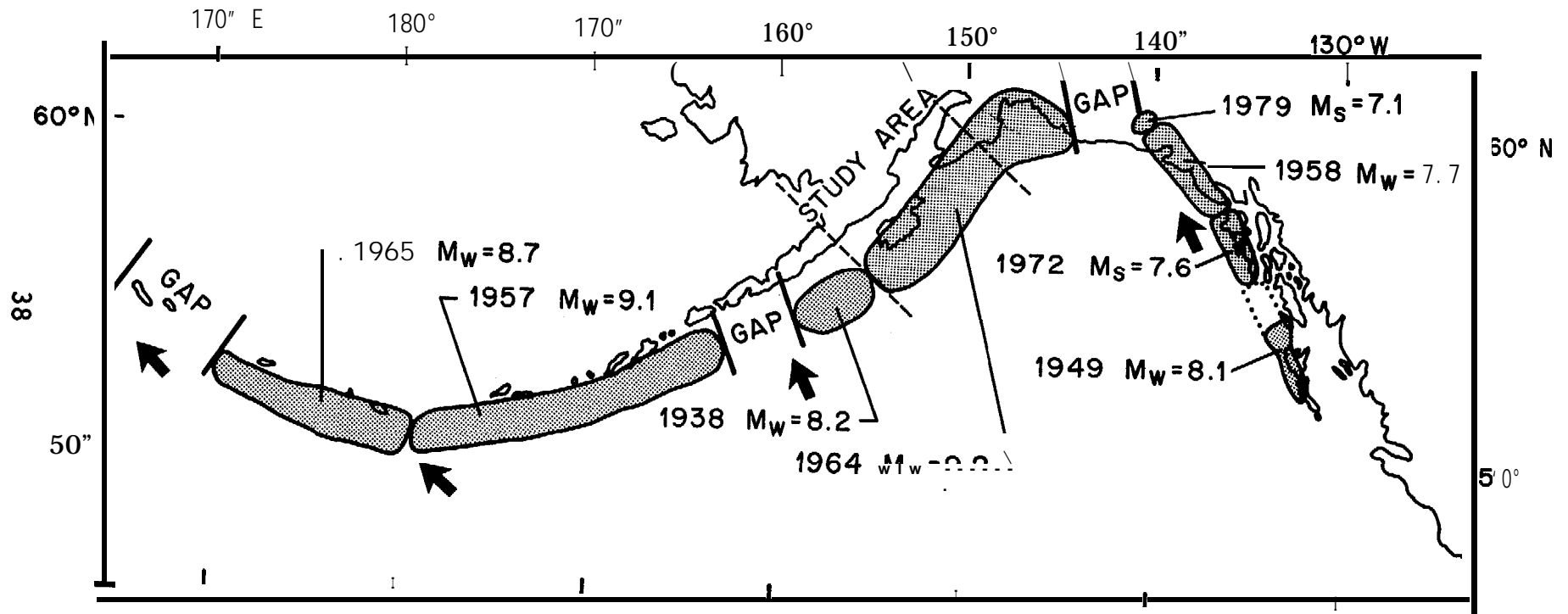


Figure 1. Aftershock zones of great earthquakes and location of seismic gaps of the Aleutian-Alaska arc system. The arrows indicate the convergence direction between the Pacific and North American plates (after Sykes et al., 1981).

Network data were also used in a variety of ways toward a better understanding of the fundamental seismotectonic processes.

Initiated as a small volcano monitoring system in Lower Cook Inlet in the early seventies, the network grew under this contract to 31 stations. The configuration is shown in Figure 2. In addition to our own stations, several stations of the USGS and NOAA's Tsunami Warning System were continuously recorded under informal data exchange agreements.

Figures 3 and 4 show, respectively, general technical layout of part of the system and characteristic system response. Each station typically consists of a **Geotech** 18300 vertical seismometer with a natural frequency of 1.0 Hz, amplifier-voltage controlled oscillator (**Monitron model 2000**), and appropriate VHF (150-165 MHz) radio gear (**Monitron T15F23** transmitters, **Monitron R15F** receivers). The stations are generally powered by "air cell" storage batteries (McGraw-Edison ST-2-1000). **Data** are being transmitted by a combination of VHF radio links and leased commercial telephone circuits. All data signals converge at a central recording facility for the system at Homer (see Figure 1). **Data** are recorded on two 16 mm, multi-channel film recorders (**Geotech Developer Model 4000**). A satellite clock (**Kinematics** True Time Division Model 468 DC) provides a common time standard and time code. System calibration is performed once a year in connection with the annual station service.

Changes in the recording media were initiated during the last years of the program when we began to record signals of 20 stations on digital tape. This type of recording involves an event detection system, developed in part under this contract, that discards non-useful portions of the recordings.

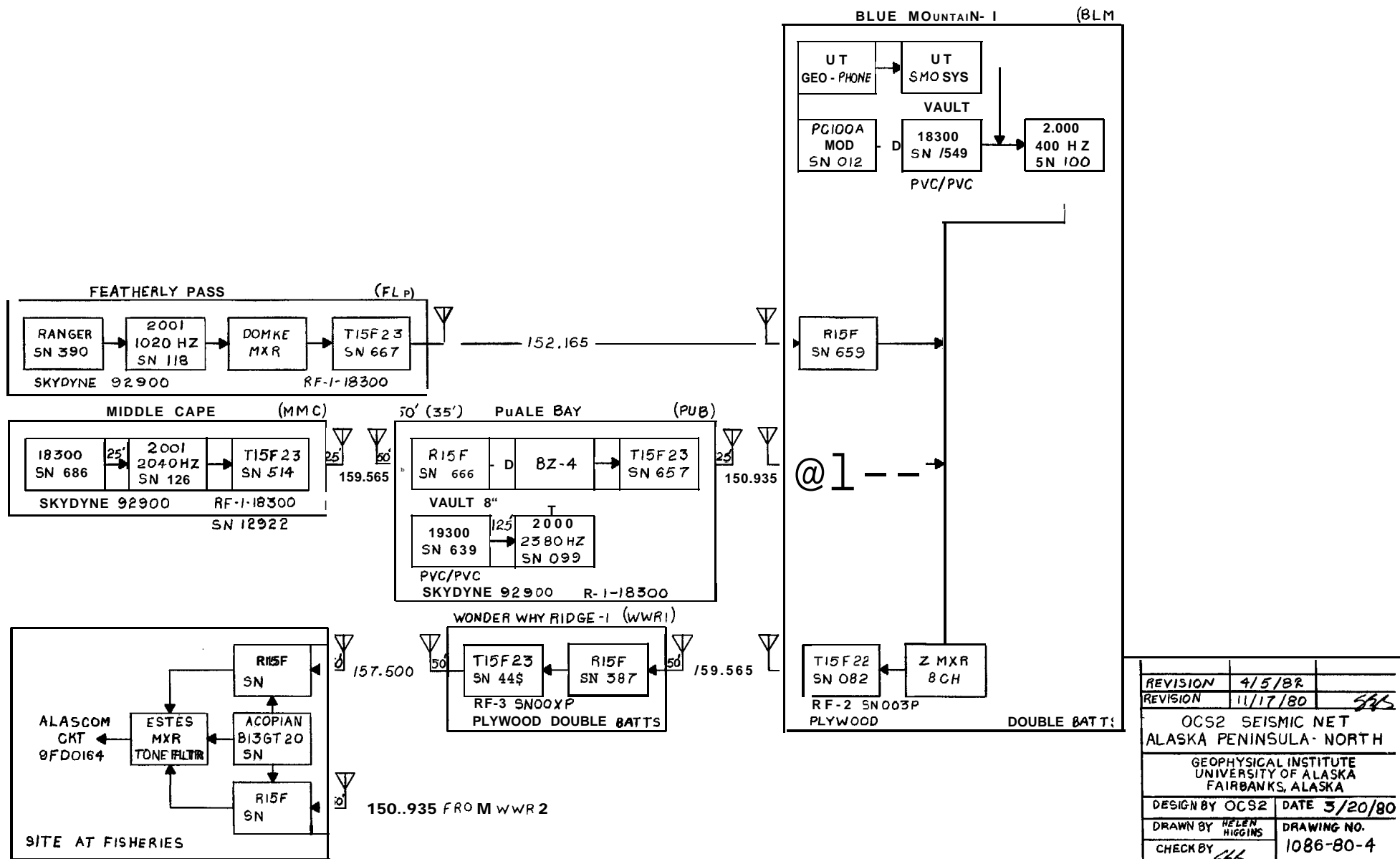


Figure 3. Typical technical layout of part of the high gain seismic network.

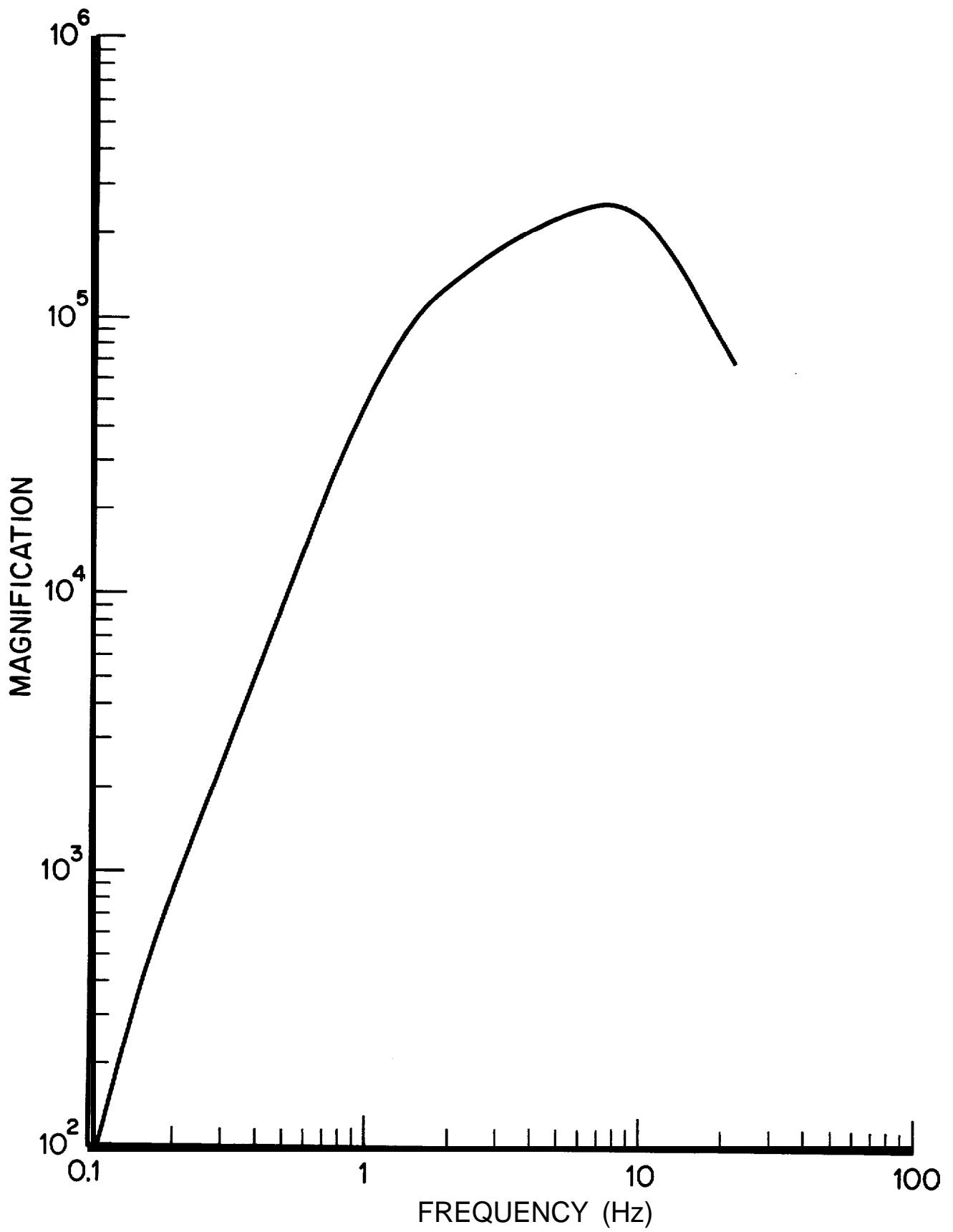


Figure 4. Typical system response of University of Alaska stations.

Routinely determined earthquake parameters are based on P-wave and S-wave arrivals. The computer program **HYPOELLIPSE (Lahr, 1980)** was used to obtain **hypocentral** parameters. Because of the large extent of the area covered by the network two different seismic velocity models were used. Travel times to stations located in the lower Cook Inlet area were calculated (regardless of the hypocenter location) for a velocity model developed by **Matumotu** and Page (1969) for the **Kenai** Peninsula area from aftershocks of the 1964 Alaska earthquake. For stations located on Kodiak Island and the Alaska Peninsula we used the model of **Engdahl** and Tarr (1970) obtained from refraction experiments in the central Aleutians. Routine magnitude determinations were based on maximum body wave trace amplitudes using Richter's (1958) local magnitude relationship, taking into account the stations system magnification value and the period of the maximum amplitude. Part of the routine data processing was the generation of epicenter maps, covering various time intervals for the different areas covered by the network. Figures **A1-A10** of Appendix 1 are epicenter plots for various time periods from 1978 through 1982.

Magnitude detection thresholds of the system varied greatly in both time and space. With respect to time, this is due to outages of up to several months, of large portions of the system in the **early** years of operation and the gradual growth of the system toward its final configuration. With respect to space, differences in detection threshold are due to variation in station density. Generally speaking, the lowest threshold is in the lower Cook Inlet area, and the highest in the area between the southwest coast of Kodiak Island and the **Semidi** Islands.

Strong-Motion Instruments

Attempts to quantify the seismic risk in the Aleutian Alaska arc system suffer from a lack of strong ground motion records. Not only is there a lack of a sufficient number of relevant records from Alaska but also from subduction zone earthquakes in general, and great ($M_s > 7.8$) subduction zone earthquakes in particular. In the U.S., thinking with respect to strong ground motion generation is strongly guided by data from California, available because of the many strong motion networks that have been installed there over the past years. But there are fundamental questions to what extent results from that seismotectonic environment can be used in Alaska. The unusually large rupture areas associated with many great subduction zone events certainly pose questions with regard to the duration and frequency content of the strong ground motion. Thus, seismic risk analysis in Alaska is faced with rather unique problems, for which results from the remainder of the U.S. can probably only serve as starting points.

The necessity of obtaining Alaskan strong motion records was recognized during the early stages of the program. We first deployed five strong motion instruments converted by us for use at remotely located Alaskan stations. We chose five locations of the high gain network (PNN, BLM, S11, SKS and UGI, Figure 1). The converted **Kinematics SMA-1** instruments were installed using the logistic support of this program. Later on in **the program, the desirability of deploying a more state-of-the-art, digital tape recording strong motion instrument, adapted** for unattended operation in the Alaskan environment, was recognized. We thus began a cooperative program with the Institute of Geophysics of the University of Texas at Austin to convert ocean bottom strong motion instruments into a

version that could be used on land in Alaska. Parts delivery problems at the University of Texas led to delays in the deployment schedule, so that by the end of the contract period only three converted instruments were deployed for one year at three remote sites (S11, CHI, UGI, Figure 1). Unfortunately, no significant strong motion records were collected during this short time of deployment.

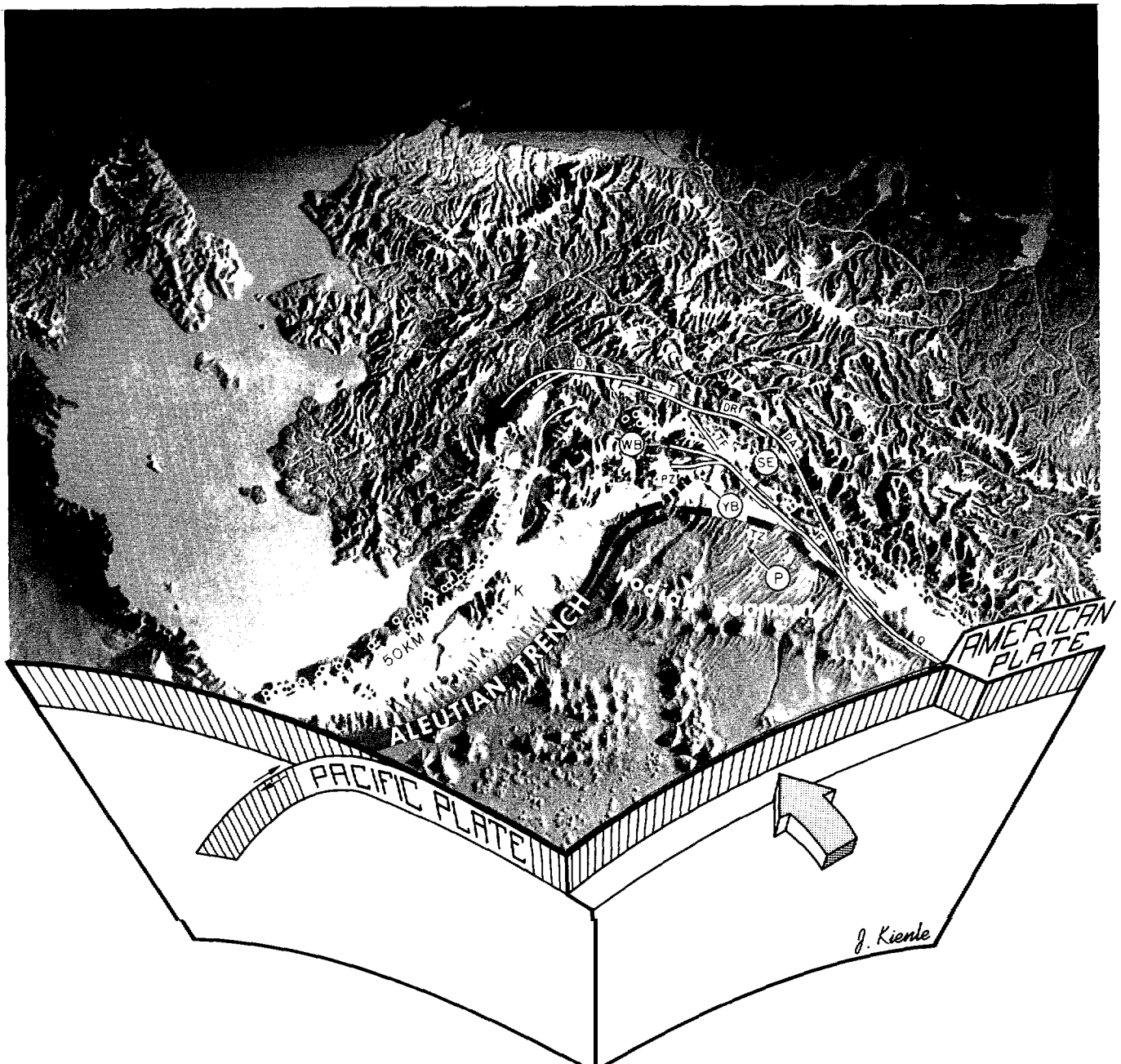
IV. RESULTS AND DISCUSSION

Seismicity and Seismic Source Zone

The tectonics of the Gulf of Alaska area are dominated by the interaction of the North American and Pacific plates (Figure 5). Along the Queen Charlotte-Fairweather fault systems the two plates are slipping past one another along a right lateral transform fault system. Along the Aleutian volcanic arc and the Aleutian-Alaska Range, up to Mt. McKinley, the oceanic Pacific plate underthrusts the continental North American plate. The Aleutian trench-axis marks the initial down-bending of the Pacific plate and the arc of active volcanoes approximately traces the **100 km** depth-contour of the subducted plate. The transition zone between these two distinct tectonic regimes lies between the **Denali** fault and the eastern Gulf of Alaska and contains a complicated system of thrust and strike slip faults. **Lahr and Plafker** (1980) **have** proposed a model where this part of the North American plate is divided into three sub-blocks (**WB, YB, SE, Figure 5**), which are partially coupled to the Pacific plate. Our particular study area (Cook Inlet and western Gulf of Alaska) is dominated by the subduction process.

Shallow Thrust Zone

The dominant source of earthquakes in our study area is the shallowly dipping interface between the underthrusting and overriding plates. The



- | | | | | | |
|----|-----------------|-------|----|--|-------|
| WB | Wrangell Block | (0.?) | D | Denali Fault | |
| SE | St. Elias Block | (0.2) | T | Totschunda Fault | (1.0) |
| YB | Yakutat Block | (5.4) | TF | Totschunda- Fairweather connecting Fault | (0,8) |
| P | Pacific Plate | (5.8) | F | Fairweather Fault | (5.2) |
| Pz | Pamplona Zone | | DR | Duke River Fault | |
| TZ | Transition Zone | | DA | Dalton Fault | (0.2) |
| | | | c | Chatham Strait Fault | |
| | | | Q | Queen Charlotte Fault | (5.8) |

Figure 5. Plate interaction in Alaska. Motion vectors of St. Elias, Yakutat and Wrangell blocks relative to North America after **Lahr and Plafker** (1980). 50 km depth contour to Benioff zone shown by solid white line. Volcanoes shown as black dots. Numbers in parenthesis after block names give rates of motion relative to fixed North American plate in **cm/yr.** Numbers in parenthesis after fault names indicate right lateral slip rate along faults in **cm/yr.**

major portion of the elastic strain accumulated along this zone by plate convergence is episodically released in the form of great ($M_s > 7.8$) earthquakes.

In our study area, the thrust zone ruptured in 1964 over an approximately 800km long section, giving **rise** to the second largest ($M_w = 9.2$) instrumentally recorded earthquake ever. Rupture lengths of that length are not unusual in the Alaska-Aleutian subduction system, the rupture lengths of the 1957 (800 km, $M_w = 9.0$) and 1965 (700km, $M_w = 8.7$) events being of similar magnitude (Figure 1). What makes the area of the 1964 event capable of producing the very largest events of the subduction system is the fact that the shallow thrust zone attains its greatest width there, producing the potentially largest rupture areas. The widening of the shallow thrust zone is associated with a general widening of the volcanic arc-trench gap from west to east. The lower edge of the large rupture zones seems to coincide with the sudden steepening of the narrow seismic zone associated with the subducting plate, which occurs at approximately 50km depth. This lower edge and the associated steepening of the active seismic zone can be interpreted as indicating the region where the subducting plate decouples from the overriding plate. Section C-C' of Figure 7, showing a projection of hypocenters into a vertical plane approximately perpendicular to the arc in the Kodiak area (see Figure 6 for location of the cross-section) shows this situation. The shallow thrust zone dips at an angle of approximately 15 degrees arcwards from the trench. The **seismicity** is primarily associated with the interface between the plates and thus maps the rupture zones of future great earthquakes. At 50km the seismic zone steepens to about 30°. This steeper zone, usually termed **Wadati-Benioff** zone (about 20 km thick as based upon the very best

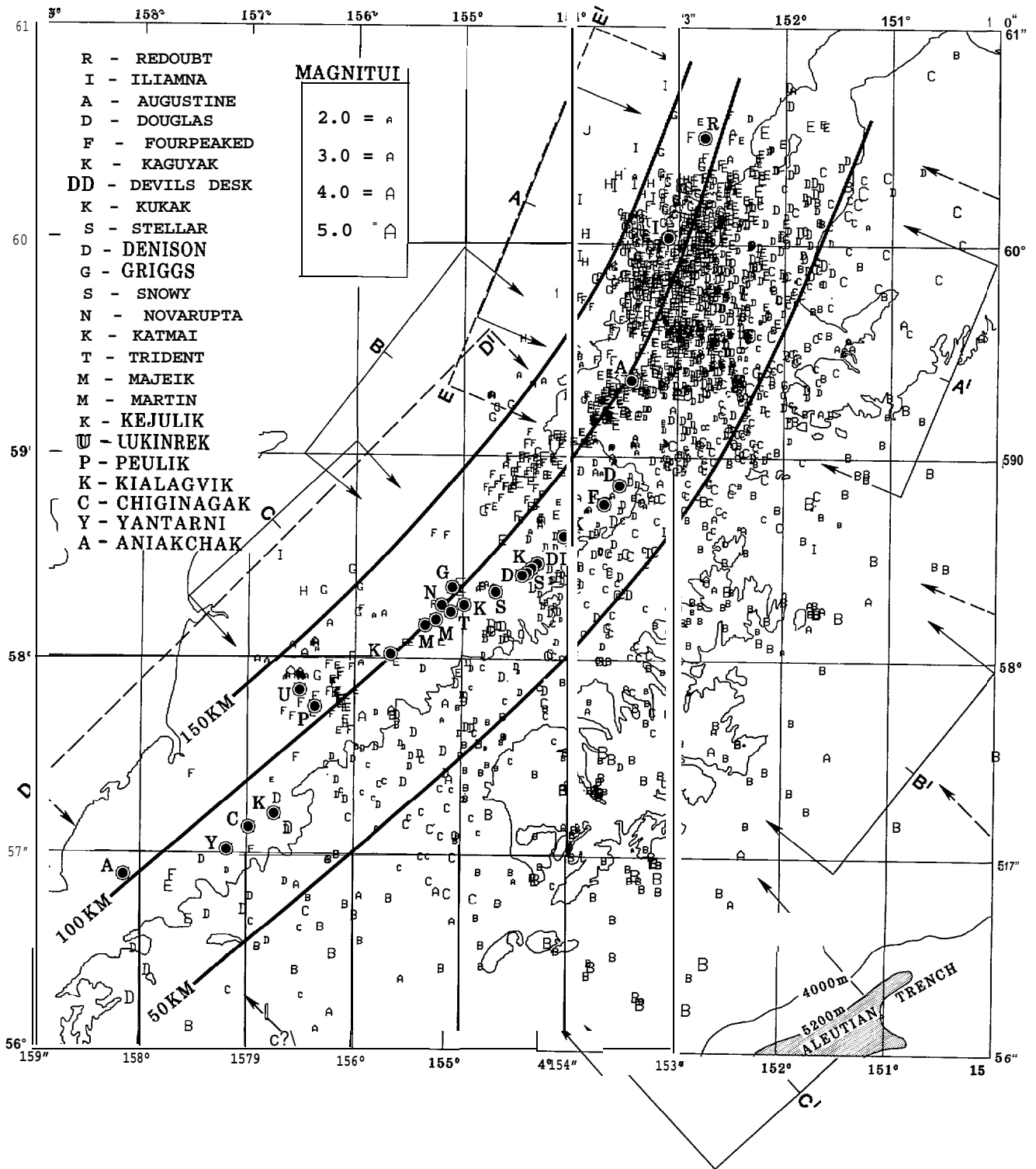


Figure 6. Epicenters, volcanoes, depth contours to top of Beni off zone (50, 100, 150 km) and location of projection volumes for cross-sections shown in Figure 7. Epicenters from local network data July 1977 to June 1981; selection criteria: recorded on at least 6 stations, RMS travel time residual ≤ 0.4 sec, relative vertical and horizontal location error ≤ 10 km. Epicenters are coded according to magnitude and depth range, A: 0-25 km, B: 26-50 km, C: 51-100 km, etc.

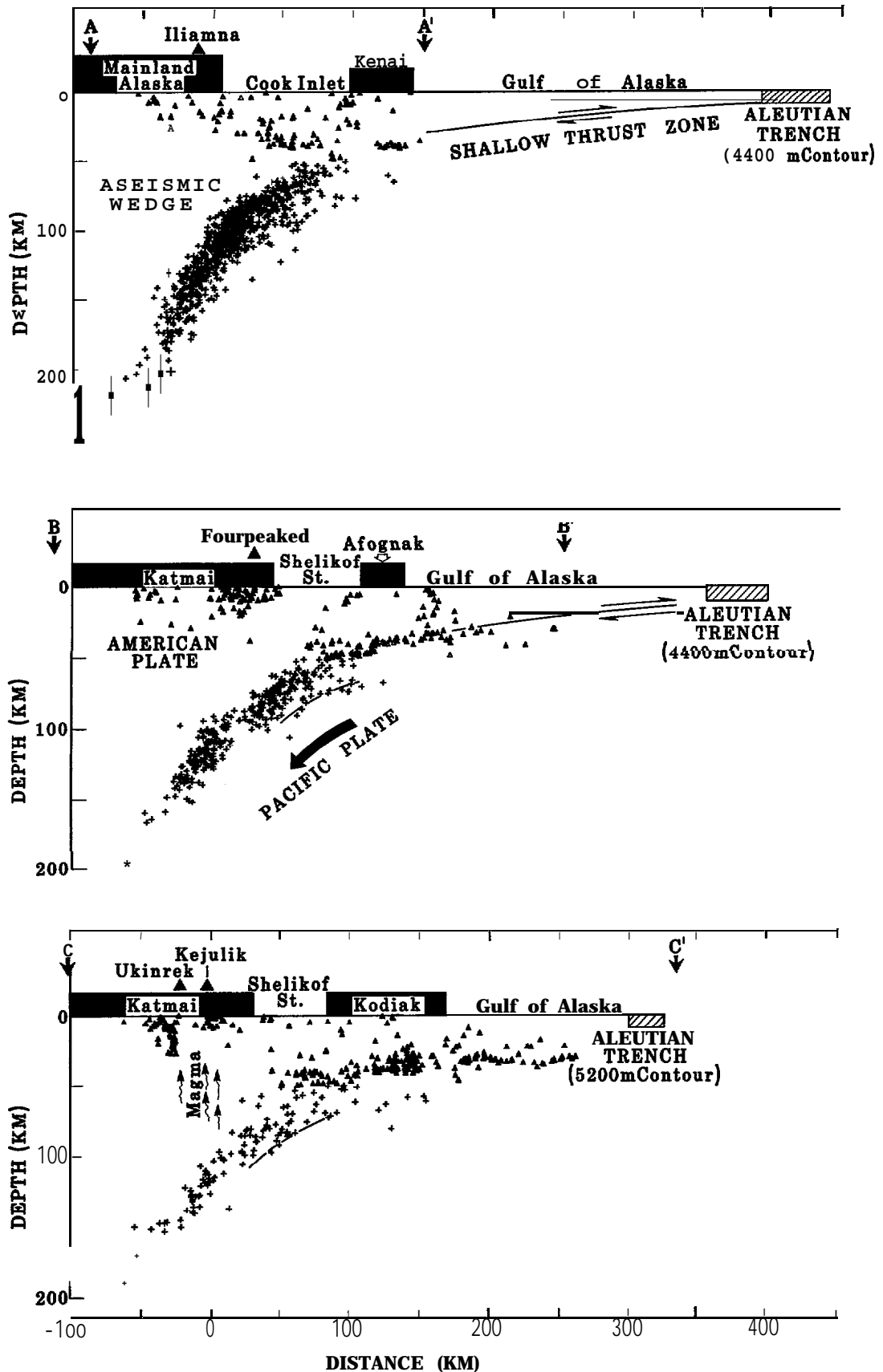


Figure 7. Cross-sectional views of Benioff zone along lines A-A', B-B', C-C' shown in Figure 6. No vertical exaggeration. Landmasses (solid black), the position of the trench, and location of volcanoes are also shown. Shallow thrust zone is added schematically. Dashed lines show possible position of second seismic zone. Selection criteria for events 0-50 km deep (triangles): recorded on at least five stations ($STA \geq 5$), relative horizontal and vertical location error (ERZ and ERH) ≤ 10 km, RMS travel time residual ≤ 0.5 sec. Selection criteria for events 50 km depth (crosses): $STA \geq 6$, ERH and ERZ ≤ 10 km, RMS ≤ 0.3 sec, and distance from epicenter to nearest station $\leq 2 \times$ depth.

hypocenter locations), represents a zone within the diving oceanic plate capable of seismic strain release. This seismic source zone, however, is not capable of producing great earthquakes and the upper magnitude limits in our area appears to be about $M_b = 6.5$.

Studies of the instrumental record (Sykes, 1971) and the historic record (Sykes et al., 1981) show that the entire Aleutian arc is capable of generating great earthquakes. The recurrence time of great earthquakes within a given segment appears to be of order 100 years. Unfortunately, the historic record as it is known so far is not sufficiently long to establish these recurrence rates within a confidence level useful for hazard analysis. The so-called seismic gap concept provides a qualitative evaluation of hazard, stipulating that those sections of the arc which have the largest time gap since the occurrence of the last great earthquake are **the** most likely ones to rupture in a great earthquake in the near future. Since the shallow thrust zone in our own study area ruptured in 1964, the greatest risk now appears to be associated with a **highly** probable great earthquake occurring in the **Shumagin** Gap; the source zone with the second highest risk is probably the rupture **zone** of the 1938 earthquake (see Figure 1). It **is** also conceivable that a rupture nucleating in the **Shumagin** Gap could propagate into the 1938 zone, and that both segments may rupture in one great earthquake.

Faults

In our study area, four major fault systems have been mapped: the Castle Mountain fault, the Bruin Bay fault, the Border Ranges fault and the Eagle River fault. These are shown for Cook **Inlet** in Figure 8. The trace of the Castle Mountain fault cuts the grain of the arc system **at** an oblique angle of 20 degrees and transects the volcano line just south of

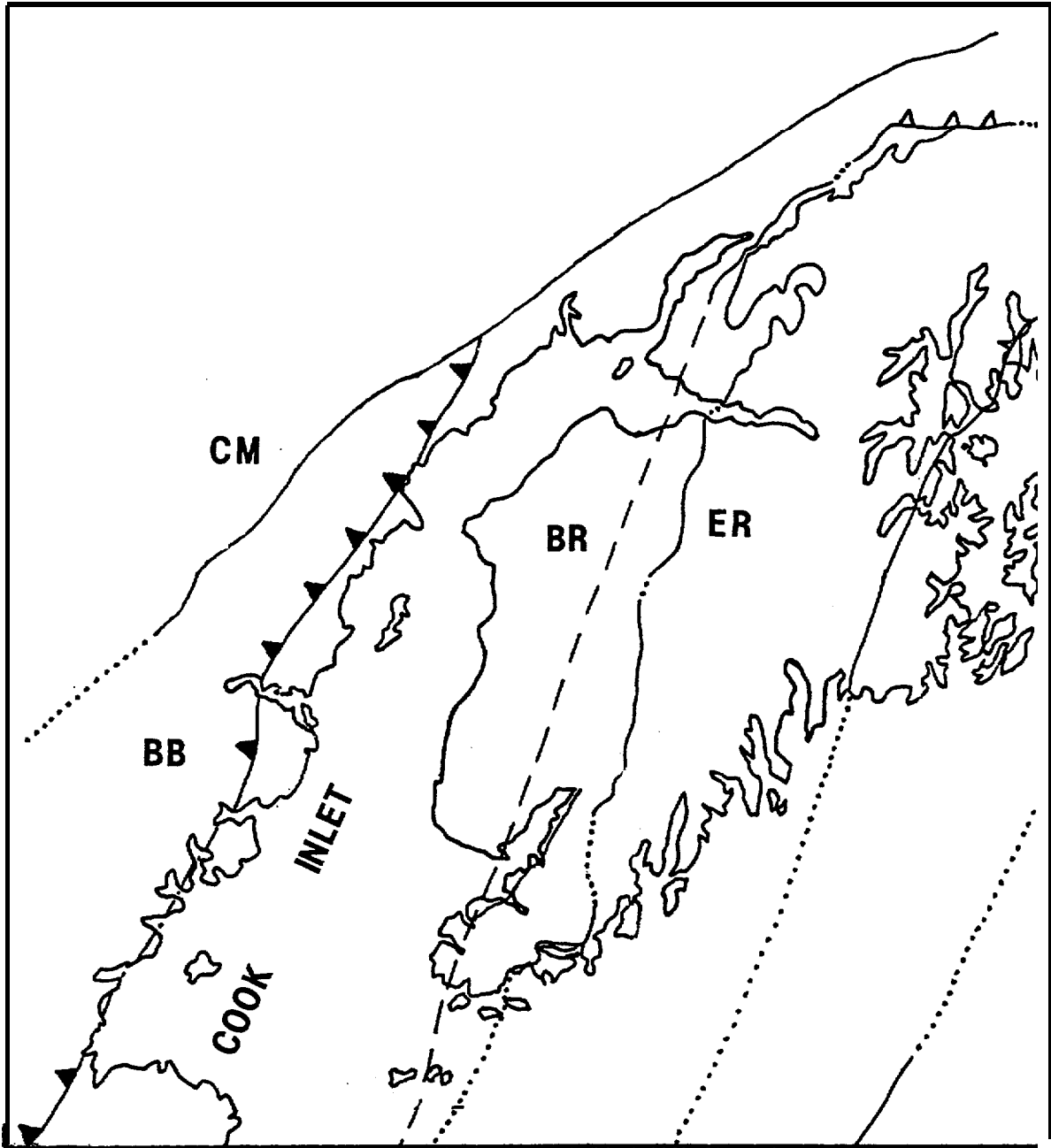


Figure 8. Fault map of the Cook Inlet area (after Beikman, 1980). BB = Bruin Bay Fault, BR = Border Ranges Fault, CM = Castle Mountain Fault, and ER = Eagle River Fault.

Mt. **Spurr** volcano. The relative motion along this fault is right lateral strike slip. Recent displacements have occurred along the Castle Mountain fault as indicated by offset Pleistocene glacial deposits and offset tectonic **lineations** (Evans **et al.**, 1972). The Bruin Bay, Border Ranges and Eagle River faults are thrusts that essentially follow the trend of the arc structure. However, none of these faults have been active since late Mesozoic-early Tertiary time and the Bruin Bay fault is not offsetting any strata younger than 25 million years (**Magoon et al.**, 1979). On Kodiak Island two major fault systems with their strike directions paralleling the arc have been mapped. The thrust system in the north (Figure 12) is the continuation of the Border **Ranges** fault system. The second, unnamed system separates Mesozoic from Cenozoic strata in the southern portion of the Island. The shallow **seismicity** is generally diffuse and is not preferentially associated with any of these faults (**Pulpan and Kienle**, 1979).

There is however a linear trend of seismic activity in the southwestern part of Kodiak Island, near the seismic station Deadman Bay (DMB on Figure 1). However, there are no mapped faults in the general vicinity of that trend, nor could we detect any tectonic **lineations** from satellite imagery.

Earthquake Activity on the Kodiak Shelf

The continental shelf off Kodiak Island is particularly active. Pulpan and **Kienle (1979)** have shown that the concentration of earthquakes between approximately **152°W** and **154°W** existed already before the 1964 Alaska earthquake. Aftershock activity in the first year following the 1964 main shock was also most pronounced in this region. Again in recent

years, since the installation of the seismic network on Kodiak Island, this portion of the shelf was the most active. The $M_s = 6.8$ earthquake of April 12, 1978 was the largest event to occur within the rupture zone of the 1964 earthquake during the past 10 years. Since the zone of intense activity based on **teleseismically** determined hypocenter locations maps out a narrow linear belt and since faulting paralleling this trend of **seismicity** had been documented (Hampton et al., 1979), it appeared of consequence for seismic hazards purposes to investigate potential relationships between the **seismicity** and the faults.

The accuracy of the **hypocentral** parameters of the earthquakes in question are different for local network solutions and for **teleseismic** solutions. The shelf events lie outside the local network, a situation that can cause location problems. On the other hand, **teleseismically** located events will be greatly influenced by the high velocity subducting slab, as the majority of rays will travel through it on account of the somewhat uneven worldwide **seismic** station distribution. In order to investigate the accuracy of locations determined by the local network for events that lie actually outside of it, we temporarily (in cooperation with RU 597) deployed a network of ocean bottom seismometers (**OBS**) on the Kodiak continental shelf. Thus the shelf events of interest could be located inside the combined land **based-OBS** network. The results of this study were:

1. Nineteen earthquakes occurring on the continental shelf of Kodiak Island were located using the combined **UA-OBS** network. At the present time, these are the best locations available for seismic activity on the Kodiak continental shelf.

2. The mean location of 15 earthquakes that could be determined with **P**-wave data from the UA network alone, shifted about 12 km when OBS data and S waves were included in the location process. However, when P- and S-wave data from more than six UA network stations were used to locate the events, the mean location fell within 1.2 km of the combined **UA-OBS** location.
3. The spatial pattern of earthquakes south of Kodiak Island recorded in this study, differs from the pattern reported by the ISC. The teleseismic epicenters are located 20 to 30 km north of epicenters determined with the combined **UA-OBS** network. The northward shift of **teleseismic** locations is probably caused by the presence of the landward-dipping subducting lithosphere. These observations are similar to the dislocations observed in the LONGSHOT experiment and other teleseismic relocation studies in the Aleutian Trench.

We also attempted to improve the locations of **teleseismically** determined events. Hypocentral parameters of these events are strongly affected by the high velocity subducting slab **on** rays that travel through it for a considerable distance. A further problem with **teleseismic** locations is the uneven azimuthal distribution of potential recording stations, with a large gap in station coverage in the Pacific Ocean **region**. Reasonable depth determination for shallow events requires the use of depth phase arrival times but during routine processing considerable error can occur due to depth phase misidentification. We therefore attempted to improve hypocentral parameters for **teleseismically** recorded events by (1) identifying depth phases from original records and (2) relocating events using the joint hypocenter determination (**JHD**) technique. We investigated thirty-six earthquakes in the magnitude range from $M_s = 5.0$ to 5.8 using

depth phases. For only **eight** of these could we identify clear phases consistent with the focal mechanism solutions at various azimuths (Figure 9). Nevertheless, these redetermined depths provide a much finer definition of the shallow thrust zone, as can be seen by comparing Figure 9 with Figure 10, which shows the location of all events based upon routine determination. The same events were **also** subjected to **epicentral** relocation by the JHD method (**Frohlich, 1979**) (Table 1). Upon relocation, the **originally** diffusely distributed events (Figure 11) collapse into two fairly narrow, **subparallel** groups (Figure 12). While the relocation provides reliable relative locations for these events, they may still be biased as a whole.

Four of the relocated events were also recorded well by our regional network. The locations of these events based on the **local** data are on the average 22 km to the south and 3 km to the west of the corresponding **teleseismic JHD** locations. This is in agreement with the results of the OBS study (Lawton et al., 1982), thus the **actual** location of the relocated **teleseismic** events is probably about 20 km to the south. Such a shift puts the events approximately along the shelf break (1000 m bathymetric contour).

Hampton et al. (1979) mapped a series of faults along the shelf break, some of them offsetting the sea floor by as much as 10 m. There is probably no direct relationship between the relocated events and these faults, but there may be an indirect one. The rigidity of the **accreted** sediments appears to be too low to permit brittle fracture at the scale indicated by the magnitude of the offsets. Focal mechanism solutions available for 11 of the relocated events (**Stauder and Bollinger, 1966**) all indicate that these events are associated with thrusting on a gently dipping

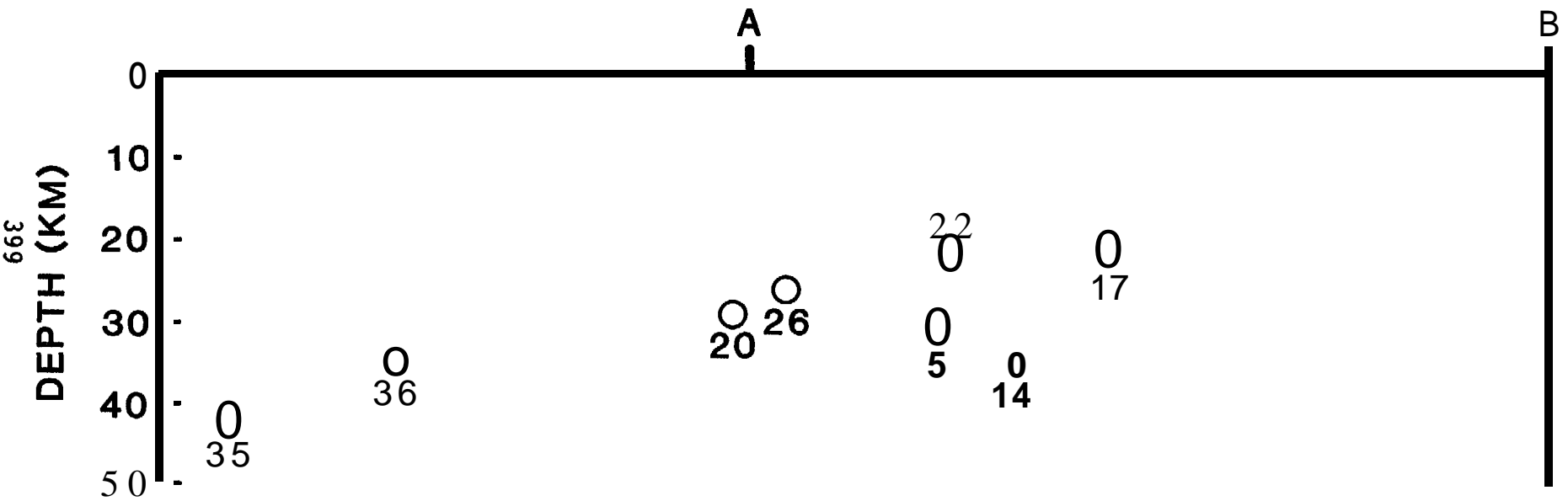


Figure 9. Depth distribution of selected events of Figure 11 for which depth phases could be well discerned on seismograms. Points A and B as in Figure 11. The numbers refer to Table 1. Events 35 and 36 were not part of the set of events which were relocated by the joint **hypocenter** determination (**JHD**) method.

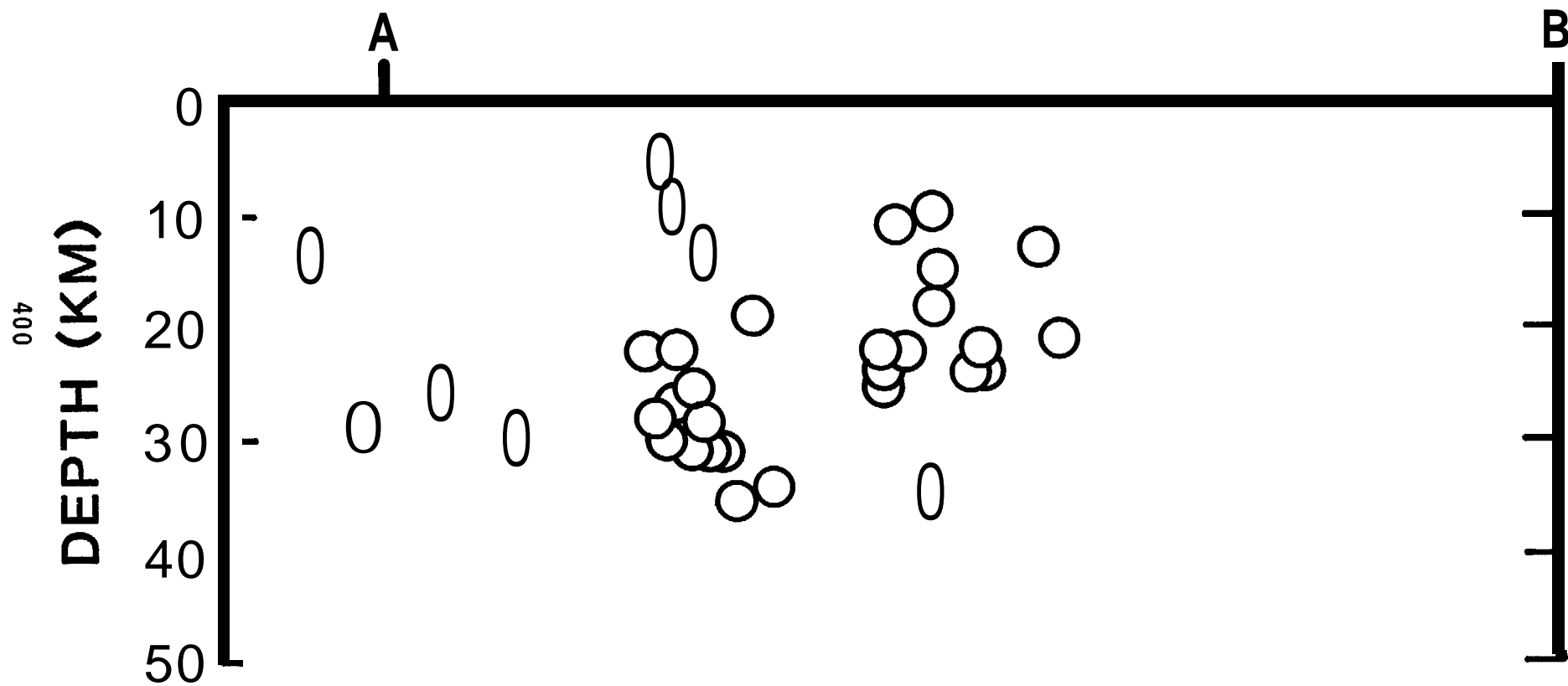


Figure 10. Depth distribution of ISC locations shown in Figure 11. **ISC** depths are based on reported depth phases. Points A and B as in Figure 10.

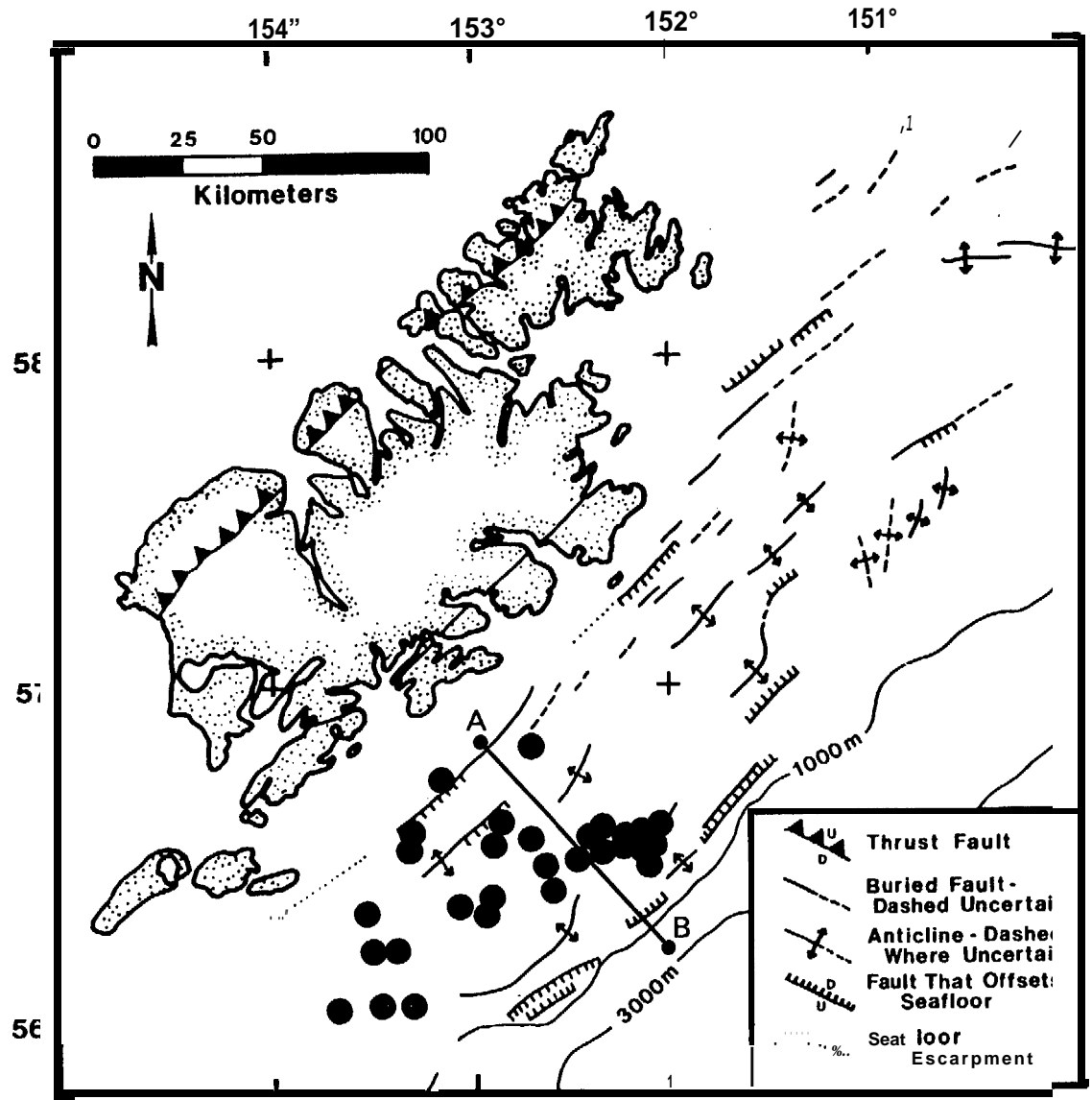


Figure 11. ISC location of 34 earthquakes that were relocated by the JHD method.

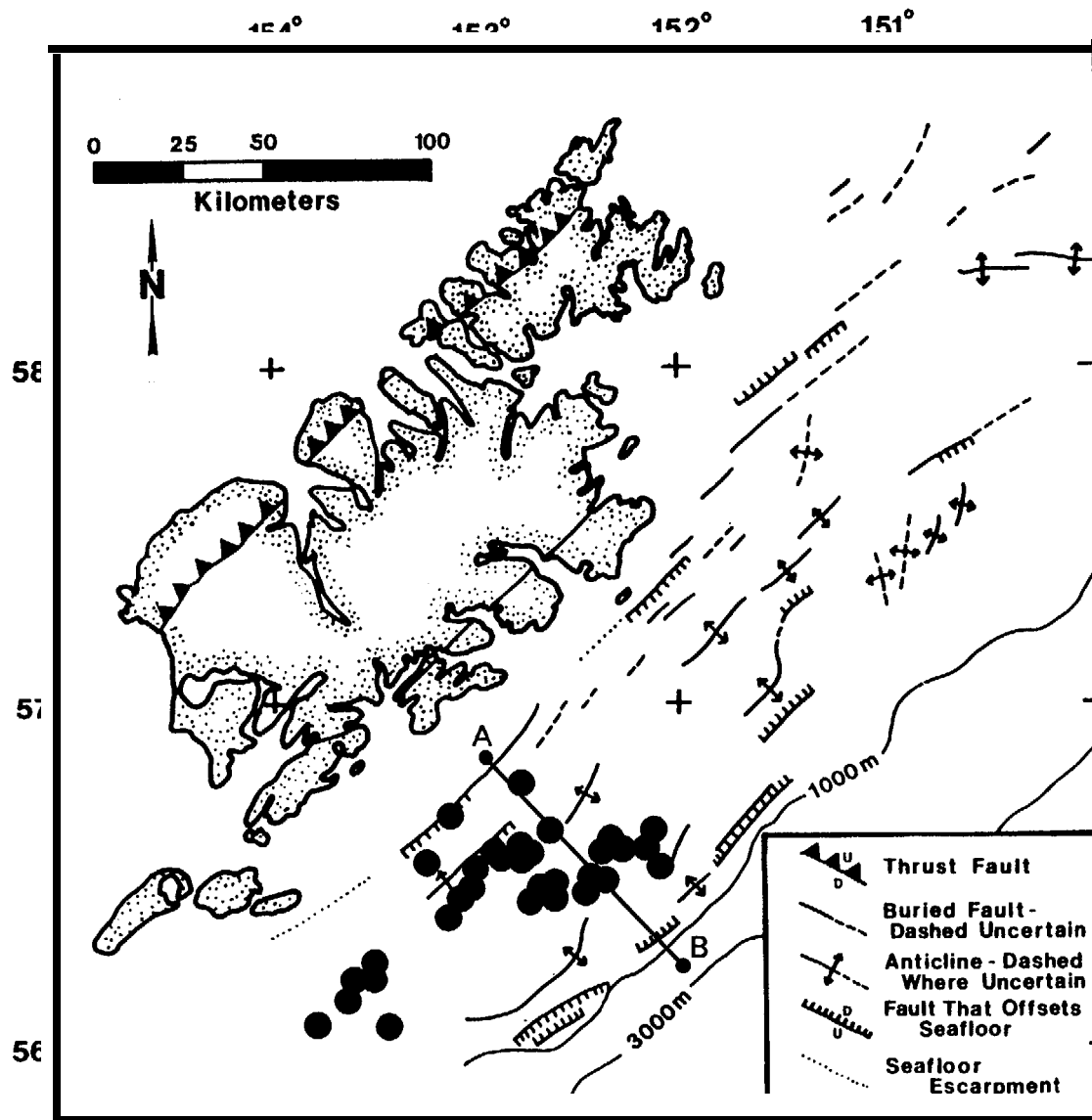


Figure 12. Location of the 34 events of Figure 11 after relocation.

TABLE 1

Locations determined by the JHD method of 34 events off Kodiak Island. In addition, the table provides the location of two events (#35 and 36) for which reliable depth phases could be identified on seismograms recorded at WSSN stations.

<u>NUMBER</u>	<u>DATE</u>	<u>LATITUDE</u>	<u>LONGITUDE</u>	<u>DEPTH</u>	<u>ORIGIN TIME</u>	<u>MAGNITUDE</u>	<u>RELIABLE DEPTH PHASES</u>
1	30 Mar 1964	56.59 N	153.00 w	22.0	0218:05.28	5.8	
2	30 Mar 1964	56.64 N	152.27 W	18.0	1609:26.99	5.7	
3	04 Apr 1964	56.60 N	152.75 W	19.0	0840:29.82	5.3	
4	04 Apr 1964	56.92 N	153.01 w	14.0	0910:54.6	5.8	
5	05 Apr 1964	56.35 N	153.48 w	30.0	0122:13.90	5.6	YES
6	05 Apr 1964	56.28 N	153.60 W	27.0	0141:43.06	5.4	
7	12 Apr 1964	56.67 N	152.33 W	22.0	0124:30.41	5.8	
8	16 Apr 1964	56.51 N	153.04 w	25.0	1926:56.08	5.5	
9	17 Apr 1964	56.53 N	153.00 w	14.0	0449:28.20	5.5	
10	06 May 1964	56.64 N	152.27 W	15.0	1526:35.99	5.5	
11	12 May 1964	56.64 N	152.35 W	11.0	1816:42.10	5.4	
12	27 Sep 1964	56.60 N	152.10 W	21.0	1550:53.41	5.4	
13	23 Jun 1964	56.64 N	152.79 W	31.0	1109:15.10	5.7	
14	22 Jan 1966	56.02 N	153.98 w	34.0	1427:07.09	5.7	YES
15	08 Apr 1966	56.69 N	152.65 W	31.00	2210:56.07	5.0	
16	11 Apr 1966	56.65 N	152.16 W	24.00	2300:22.41	5.0	
17	09 May 1967	56.53 N	152.60 W	22.00	1236:36.24	5.0	YES
18	13 May 1967	56.51 N	152.71 W	23.00	0518:54.21	5.0	

404

<u>NUMBER</u>	<u>DATE</u>	<u>LATI TUDE</u>	<u>LONGI TUDE</u>	<u>DEPTH</u>	<u>ORI GI N TIME</u>	<u>MAGNI TUDE</u>	<u>RELI ABLE</u>	<u>DEPTH</u>	<u>PHASES</u>
19	29 Jan 968	56.32 N	153.51 w	6.0	2052:20.75	5.2			
20	22 Dec 968	56.39 N	154.07 w	29.0	1644:43.81	5.4		YES	
21	20 Nov 969	56.61 N	153.23 W	30.0	2346:10.57	5.2			
22	21 Nov 1969	56.31 N	153.56 W	22.0	0014:10.71	5.1		YES	
23	24 Nov 1969	56.17 N	153.77 w	28.0	2251:48.47	5.4			
24	12 Jan 1970	56.71 N	152.13 W	35.0	0454:31.93	5.3			
25	20 Sep 1971	56.45 N	153.15 w	30.0	0644:13.65	5.1			
26	18 Jan 1972	56.75 N	153.12 W	26.0	0017:44.95	5.1		YES	
27	01 Aug 1974	56.56 N	152.36 W	23.0	0555:36.11	5.1			
28	01 Aug 1974	56.55 N	152.58 W	22.0	0759:54.92	5.1		-	
29	01 Aug 1974	56.56 N	152.45 W	10.0	0507:59.81	5.3		-	
30	07 Aug 1974	56.62 N	152.75 W	35.00	0823:36.26	5.0			
31	22 Ott 1976	56.17 N	153.42 W	24.0	1835:25.19	5.5			
32	10 Aug 1977	56.63 N	152.89 W	28.0	0935:57.55	5.1			
33	12 Apr 1978	56.62 N	152.87 W	10.0	0342:03.51	5*7			
34	12 Apr 1978	56.52 N	152.43 W	22.0	0522:29.90	5.0			
35	11 Mar 1970	57.39 N	153.97 w	42.0	2238:32.4			YES	
36	22 Aug 1973	57.09 N	154.12 W	36.0	1814:36.6			YES	

plane. Although the ambiguity in first motion fault plane solutions also permits dip slip faulting on a steeply dipping plane, the direction is opposite to that generally inferred for **imbricate** faults of the **accretionary** wedge, which appears to be **aseismic** (Chen et al. , 1982). However, the relationship between the activity along the main thrust plane of the subduction zone and the observed faults might **follow** the model suggested by Fukao (1979). The majority of the events relocated in this study are part of the aftershock sequence of the 1964 Good Friday Alaskan earthquake. The relatively narrow belt of aftershock **seismicity** evident from our relocations probably reflects the brittle fracture release of stress concentrations associated with leading seaward edge of the shallow dipping rupture zone of the main shock. Since, according to Fukao's (1979) model , the main rupture does not propagate **all** the way toward the trench along the interface between the overriding and underthrusting plates, the wedge-shaped region of sediments between the trench axis and the leading edge of the rupture zone will be heavily stressed. These stresses will be relieved mostly in a ductile manner along **slip** lines curving from the tip of the main rupture zone upwards and emerging at steep dip angles on the ocean floor, generating the mapped sea floor offsets noted by Hampton et al. (1979).

Intermediate Depth Earthquake Activity

Earthquake activity below 50 km is exclusively associated with a well defined **Benioff** zone. While this deeper seismic source zone has much lower seismic energy release potential than the shallow thrust zone, study of its **seismicity** and precise location of earthquakes can provide important information concerning the details of the subduction process. For example, several recent studies have focused on earthquake locations

within subducted lithosphere and have apparently identified a second weaker zone of **seismicity** beneath the planar **Benioff** zone (**Fujita** and **Kanamori**, 1981). The combination of the usual Benioff zone together with this lower less active zone is known as a "double Benioff zone." This has been clearly observed in Japan (**Hasegawa** et al., 1978a, 1978b). and observed less clearly in several other areas (e.g, **Veith**, 1974; **Lahr**, 1975; **Samowitz** and **Forsyth**, 1981; **Reyners** and **Coles**, 1982). In addition, detailed delineation of the geometry of the **Benioff** zones from the spatial **distribution of accurately determined earthquake hypocenters is important** in **determining** the extent and nature of the lateral segmentation of the subducted **lithosphere** (**Isacks** and **Barazangi**, 1977). These lateral segment boundaries might control the extent of the rupture surface during great earthquakes (**McCann** et al., 1979; **Davies** and **House**, 1979; **Davies** et al., 1981). Finally, the relationships between arc volcanism and the configuration of the subducting plate have been topics of several studies (**Stoiber** and **Carr**, 1973; **Carr** et al., 1973; **Isacks** and **Barazangi**, 1977; **Jacob** et al., 1977; **Kienle** et al., 1983).

There are several features of the **Alaska Benioff** zone near Kodiak Island and Cook Inlet which suggest that the subducted plate is laterally deformed or segmented. First, the generally SW-NE striking line of volcanoes appears to undergo an abrupt change to a more northerly trend near 59°N (Figure 6). A distinct increase in the rate of seismic activity at intermediate depths occurs in Cook Inlet, just to the north of this change. Still further north, at about **63°N**, the intermediate depth earthquake zone once again bends to a more easterly strike, and terminates east of Mt. **Denali** at **64.1°N** (**Tobin** and **Sykes**, 1966; **VanWormer** et al., 1974; **Davies**, 1973; **Agnew**, 1979).

We used the **JHD** method to relocate 341 well recorded events with focal depths greater than about 40 km that occurred between **56.5°N** and **60.5°N**, and between **151.6°W** and **156.5°W** (Figure 13). These relocated hypocenters show that the **Benioff** zone has a dip of about 45°, its thickness varies from about 15 km in the southwestern area to about 25km in the northeastern section (Figure 14). The strike of the **Benioff** zone changes by about 15° from the southern to the northern group of events. In the cross-section displaying the northern group of events, we see several events falling well below the **Benioff** zone. One of these events was one of the best recorded ones, so we believe their relative location to be real.

First motion focal mechanism solutions which we have obtained for twenty earthquakes (Table 2) in the Lower Cook Inlet region show that at intermediate depth the sinking slab between **59.5°N** and **61°N** is under horizontal north-south compression (Figure 15; Table 3 and 4). The focal mechanism solution obtained for one of the events below the main **Benioff** zone gave stress orientations quite different from the other solutions (Figure 16). Since differences in the principal stress directions between the upper and lower zone is characteristic for double **Benioff** zones, one could interpret the lower events as being part of a double **Benioff** zone.

Relying primarily on the observed change in strike and apparent thickness of the **Benioff** zone, one can interpret these data also to suggest that the subducted lithosphere separates into two distinct segments as it bends and subducts beneath Cook Inlet. Because the direction of subduction is not perpendicular to the volcanic arc the events situated beneath the **Benioff** zone in Cook Inlet may be part of the southwestern plate segment.

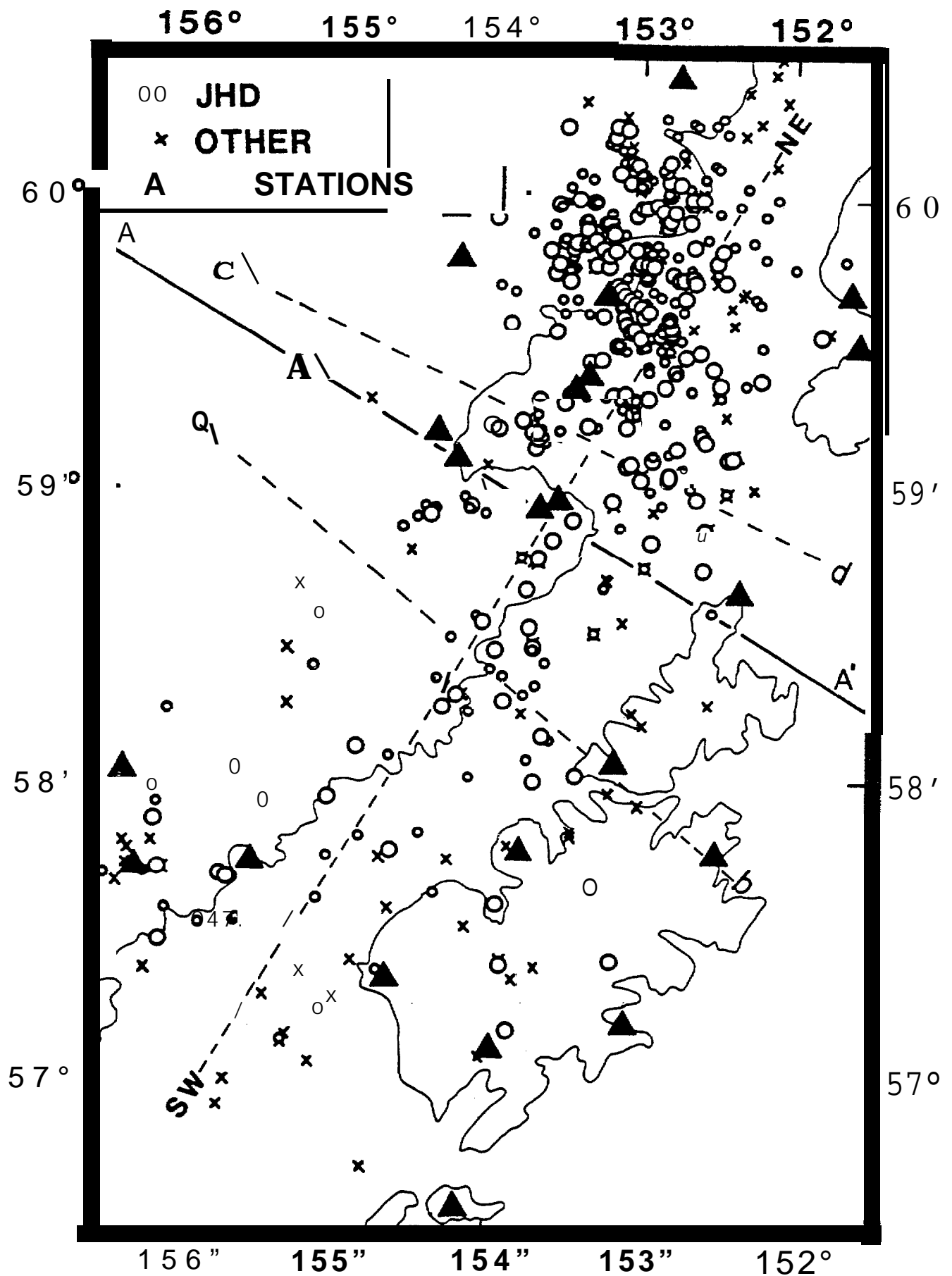


Figure 13. Epicenters of earthquakes relocated by the JHD method using regional network data. Large circles are highest quality events, smaller circles low quality events. X's are events located using station corrections determined by the JHD method.

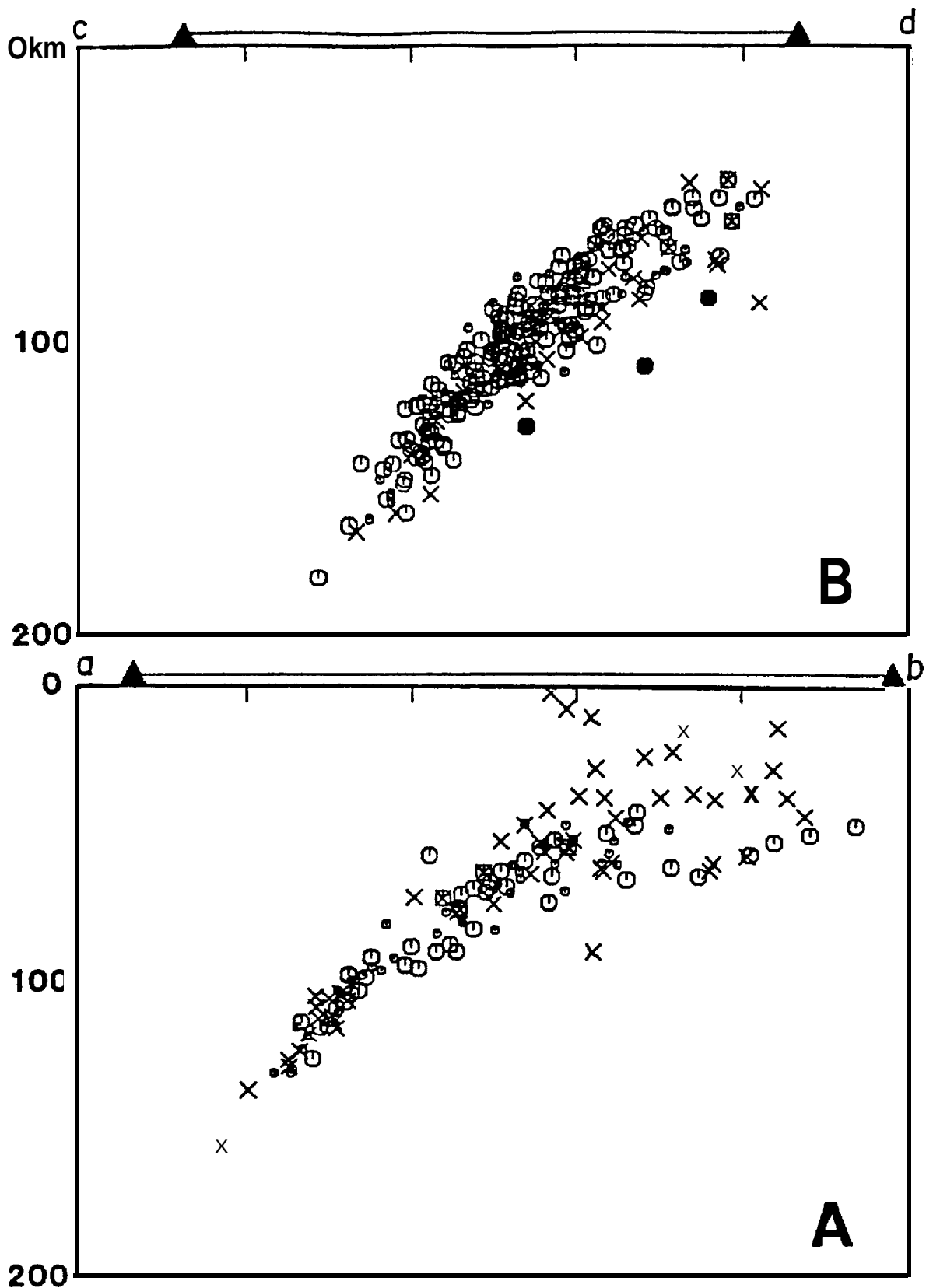


Figure 14. Cross-section of seismic events mapped in Figure 13. Section A has a trend of 50°W of N and includes events in the southwestern portion of Figure 13 (S of line A-A'). Section B has a trend of 65°W of N, and includes events in the northwestern portion of Figure 13 (N of line A-A'). In section B, note especially that a few of the events (denoted by filled circles) lie **distinctly** beneath the main Benioff zone.

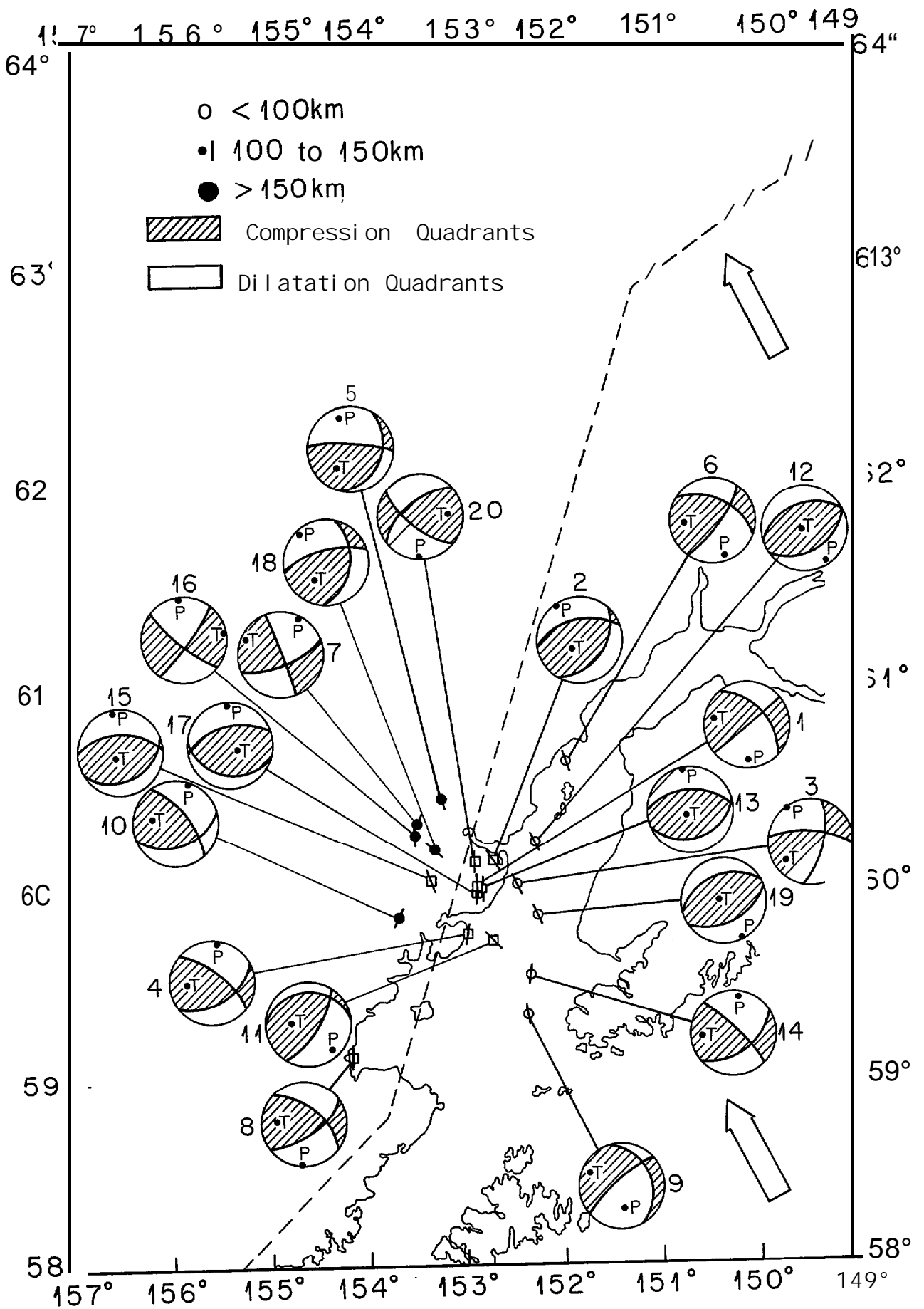


Figure 15. First motion fault plane solutions of Benioff zone events in Lower Cook Inlet.

TABLE 2

Date and locations of events for which the first motion fault plane solutions shown in Figure 14 were obtained.

Event Number	Date	<u>Hr. Min. Sec</u>	Depth (km)	<u>Latitude</u>	<u>Longitude</u>
1	Jan 25, 79	19 30 07.76	112.6	60°00.08N	152°51.47W
2	Feb 01, 79	12 29 06.24	119.9	60°08.39N	152°43.54W
3	Feb 09, 79	18 49 26.29	83.8	60°00.87N	152°28.37W
4	Mar 07, 79	12 10 37.45	107.6	59°40.58N	152°59.34W
5	Apr 04, 79	02 34 25.93	185.1	60°26.63N	153°13.09W
6	Apr 04, 79	04 51 37.77	91.9	60°30.79N	151°57.57W
7	Apr 04, 79	08 16 14.54	205.9	60°19.58N	153°27.22W
8	Apr 15, 79	11 10 39.22	129.9	59°07.17N	154°09.45W
9	Apr 20, 79	08 42 32.96	75.9	59°19.97N	152°21.42W
10	Jul 04, 79	08 15 38.96	150.1	59°50.13N	153°40.10W
11	Aug 15, 79	18 30 59.20	101.6	59°43.62N	152°43.60W
12	Jan 01, 80	07 03 30.84	93.1	60°13.45N	152°15.96W
13	Jun 03, 80	10 59 26.81	108.1	60°00.35N	152°49.34W
14	Jun 11, 80	04 38 06.38	59.3	59°33.38N	152°19.59W
15	Jun 15, 80	19 01 53.37	148.0	60°02.29N	153°20.39W
16	Jun 17, 80	09 16 11.45	193.8	60°16.07N	153°28.92W
17	Aug 12, 80	14 44 30.90	104.2	59°59.14N	152°52.61W
18	Sep 05, 80	05 46 13.73	167.4	60°12.25N	153°17.43W
19	Sep 13, 80	07 24 14.26	95.2	59°51.69N	152°14.81W
20	Sep 21, 80	21 00 19.39	122.5	60°08.30N	152°54.17W

TABLE 3

Nodal plane parameters for the events of **Table 2**

<u>Event Number</u>	<u>Plane 1</u>			<u>Plane 2</u>		
	<u>Dip Direction</u>	<u>Angles (degrees)</u>		<u>Dip Direction</u>	<u>Angles (degrees)</u>	
		<u>Dip</u>	<u>Slip</u>		<u>Dip</u>	<u>Slip</u>
1	149	88	39	49	52	03
2	129	46	66	343	50	64
3	104	67	22	05	70	24
4	40	70	44	148	49	28
5	03	80	62	112	29	22
6	27	50	16	128	78	42
7	69	87	21	159	70	02
8	40	59	28	144	66	34
9	317	78	58	68	34	24
10	51	68	44	161	50	30
11	352	30	44	122	70	66
12	337	42	87	150	43	85
13	357	52	81	161	38	78
14	46	80	37	142	54	14
15	356	55	79	156	35	74
16	219	79	03	143	83	11
17	343	58	72	193	36	74
18	346	69	48	96	46	28
19	338	40	86	153	50	87
20	321	60	23	219	70	33

TABLE 4

Stress axes parameters for the events of **Table 2**

Event Number	P Axes		T Axes		B Axes	
	Trend (Degrees)	Plunge	Trend (Degrees)	Plunge	Trend (Degrees)	Plunge
1	178	24	283	27	52	52
2	330	03	59	71	327	19
3	324	01	234	30	57	60
4	08	12	266	45	110	43
5	342	30	212	48	88	28
6	161	18	266	38	51	48
7	26	12	292	16	151	70
8	180	04	275	40	85	50
9	170	48	294	26	40	32
10	18	10	279	46	120	42
11	138	22	271	59	40	22
12	154	01	260	86	64	04
13	350	07	224	80	81	07
14	09	16	288	33	121	53
15	349	10	218	77	81	10
16	353	14	83	02	177	78
17	355	11	121	72	262	14
18	316	13	211	49	58	40
19	156	06	309	84	65	02
20	181	06	86	37	281	53

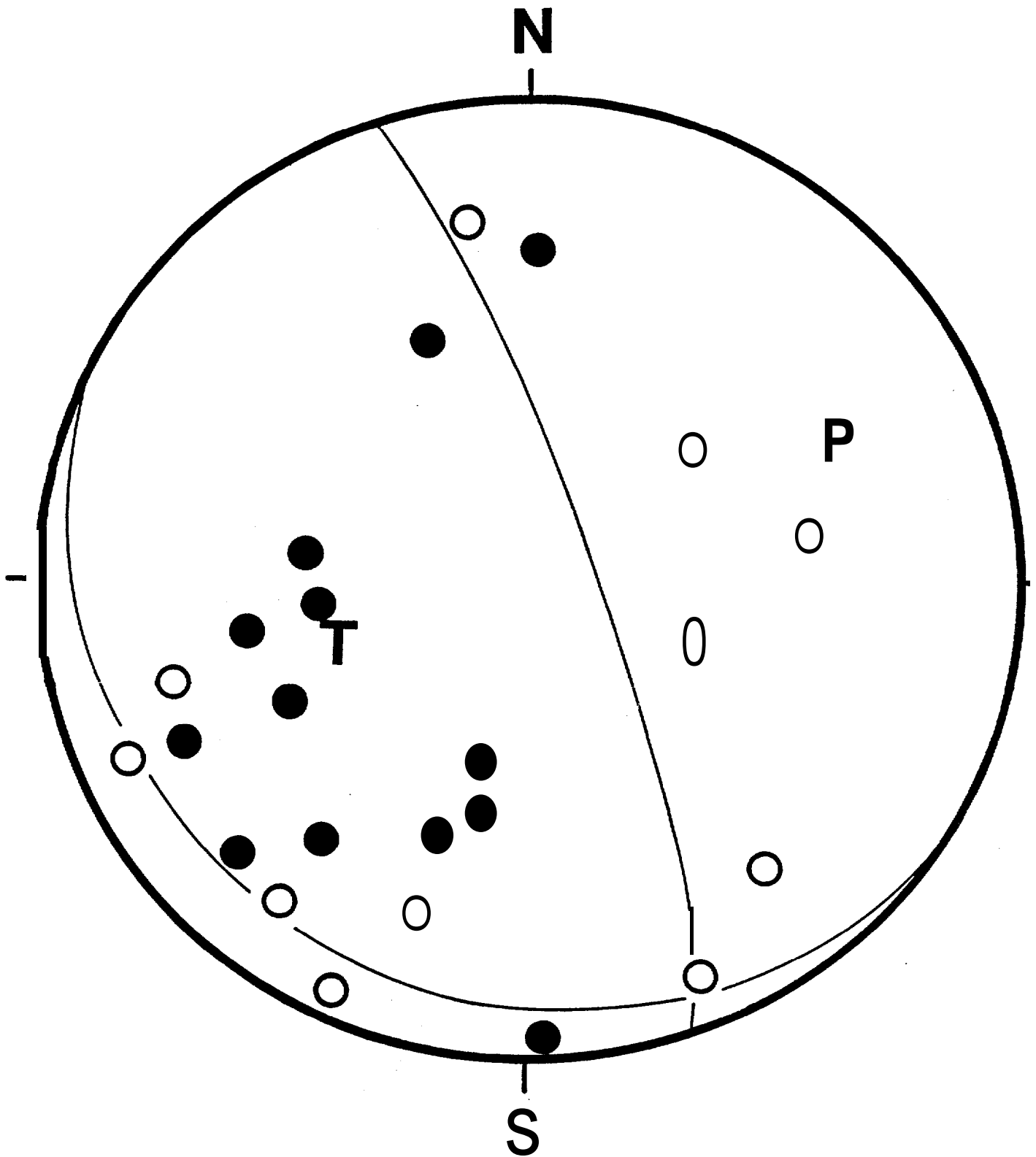


Figure 16. First motions (open circles for dilatations, full circles for compression) of one of the events situated below the main Benioff zone in Lower Cook Inlet. Note that the P and T axes differ in their orientation from those in Figure 15.

Seismic Exposure Studies

A seismic exposure study for the Gulf of Alaska region was made during the OCSEA program. The study was conducted **by Woodward-Clyde** Consultants with participation of the various OCSEAP Principal Investigators involved in seismic hazard studies in that area (Woodward-Clyde Consultants, 1982). **Woodward-Clyde** had also conducted the so-called "OASES" study (**Woodward-Clyde** Consultants, 1978), the first comprehensive seismic risk analysis of Alaskan offshore regions. The OCSEAP study was to update the OASES study by incorporation of the concept **of** seismic gaps into the analysis and by revision of the **characterization** of the seismic source zones on the basis of the most recent data.

Unfortunately, the **Woodward-Clyde** study was completed only when OCSEAP was coming to an end. Thus, while Principal Investigators participated in two workshops to discuss and specify the input data, there was no possibility to perform the crucial sensitivity studies as to how various assumptions concerning the input data would influence the exposure values. This is especially true with respect to the various transition probabilities and holding times for great earthquakes, when the occurrence of the latter is modeled as a **semi-Markov** process. Also, the presently available updated historic record (Davies et al., 1981) should be incorporated into specifying the initial states in the **semi-Markov** process. The exposure values are presently based upon distance-magnitude relationships that incorporate only few Alaskan data; the influence of changing these relationships needs to be studied.

V. CONCLUSIONS

The seismic hazard of the Aleutian-Alaska arc system is dominated by the **occurrence** of great earthquakes ($M_s > 7.8$) along the interface between

the subducting Pacific plate and the overriding North American plate. In our study area, along the arc from the **Semidi** Islands to Lower Cook Inlet, data from a network of seismograph stations operated during the course of this study delineate this interface with very good spatial resolution. The interface attains its greatest width in this and the easternmost section of the arc, making these areas the ones capable of generating the largest events of the arc system. However, since the recurrence interval for great earthquakes in the arc system is in the order of 100 years and the last one occurred in our study area only 20 years ago (in 1964), the greatest exposure in the near future is most likely associated with a great earthquake in one or both of the two seismic gaps identified to the east and west, respectively, of our study area (figure 1). In the case of the rupture of the **Shumagin** gap in a great earthquake it is possible that this rupture spreads into the 1938 rupture zone, the two sections breaking in a single great earthquake.

Other seismic source zones have been delineated with good resolution too, but none of these approach the **seismogenic** potential of the interface thrust zone.

While the results of this study provide a good quantitative description of source geometries and source potentials, two important aspects presently limit the usefulness of seismic exposure calculations: the uncertainties in predicting the time of occurrence of a great earthquake in a particular section of the arc and in predicting the characteristics of the ground motion generated at a particular site as a consequence of such an earthquake. The seismic gap concept provides a rational but only qualitative concept of likelihood of occurrence of a great earthquake. But all methods of projecting recurrence intervals on the basis of the historic record will suffer from the fact that it is too short to provide a sufficient number of cycles for a statistically

meaningful estimate. Our knowledge of the mechanical nature of the fault **zone** and spatial variations thereof is presently too limited for predictions, based on the plate convergence rates along the arc, **to** be more than rough guidelines for establishing recurrence intervals. Thus all statistical recurrence estimates for the great earthquakes which dominate the seismic hazard, presently contain large uncertainties.

Our ability to predict strong ground motion at a site is strongly linked to our knowledge of the details of the rupture process of an earthquake and the modification of the generated motion during propagation towards a particular site. The limited number of strong motion records available from subduction zone earthquakes generally, and from Alaska in particular, prevents testing of various theoretical models of the rupture process against actual data. Similarly the data are insufficient to generate with reasonable confidence empirical relationships describing the attenuation of strong ground motion with distance?. The exposure calculations performed under the OSCEAP program suffer from these deficiencies. Thus strong ground motion data and seismological studies towards the mechanical nature of the plate interface and the rupture process would be of the greatest benefit for seismic risk studies of the Alaska-Aleutian arc system.

VI. REFERENCES

- Agnew, J. **Seismicity** of the central Alaska Range, Proc. Alaska Sci. Conf., 30, 73, 1979 (abstract).
- Beikman, H. M., Geological Map of Alaska, U.S. Geol. Survey, 1980.
- Carr, M. J., Stoiber, R. E., and C. L. Drake, **Discontinuities** in the deep seismic zone under the Japanese arc, Bull. Geol. Soc. Amer., 84, 2917-2930, 1973.
- Chen, A. T., C. Frohlich, and G. V. Latham. **Seismicity** of the forearc marginal wedge, J. Geophys. Res., 87, 3679-3690, 1982.
- Davies, J. N. and L. House, Aleutian subduction zone **seismicity, volcano-trench separation**, and their relation to great thrust-type earthquakes. J. Geophys. Res., 84, 4583-4591, 1979.
- Davies, J., L. Sykes, L. House, and K. Jacob, **Shumagin** seismic gap, Alaska Peninsula: History of great earthquakes, tectonic setting, and evidence for high seismic potential, J. Geophys. Res., 86, 3821-3855, 1981.
- Engdahl, E. R. and A. A. Tarr. Aleutian **seismicity, Milrow** seismic effects, U.S. Coast and Geodetic Survey, CGS-746-102, 1970.
- Evans, C. D., F. H. Buck, R. T. Buffler, S. G. Fisk, R. B. Forbes, and W. B. Parker, The Cook Inlet--An Environmental Background Study of Available Knowledge, prepared by the University of Alaska, Resource and Science Service Center, Alaska Sea Grant Program, Anchorage, Alaska, for the Alaska District Corps of Engineers, Anchorage, Alaska, 446 pp., 1972.
- Frohlich, C., An efficient method for joint hypocenter determination for large groups of earthquakes, Computer and Geosciences, 5, 387-389, 1979.

- Fujita**, K. and H. **Kanamori**, Double seismic zones and stresses of intermediate depth earthquakes, Geophys. J., 66, 141-156, 1981.
- Fukao, Y., Tsunami earthquakes and subduction processes near deep-sea trenches, J. Geophys. Res., 84, 2303-2314, 1979.
- Gedney, L., Tectonic stresses *in* southern Alaska in relationship to regional **seismicity** and new global tectonics, Bull. Seismol. Soc. Amer., 60, 1789-1802, 1970.
- Hampton, M. A., A. M. **Bouma**, R. Von Huene, and H. **Pulpan**, Geo-Environmental Assessment of the Kodiak Shelf, Proc. Offshore Tech. Conf., April 30-May 3, 1979, Houston, Texas, 1, 365-376, 1979.
- Hasegawa**, A., N. **Umino**, and A. **Takagi**. Double-planed structure of the deep seismic zone in the northeastern Japan arc. Tectonophysics, 47, 43-58, 1978.
- Hasegawa, A., N. **Umino**, and A. **Takagi**, Double planed deep seismic zone and upper mantle structure *in* the northeast Japan Arc, Geophys. J., 54, 281-296, 1978.
- Jacob, K. H., K. **Nakamura**, and J. N. Davies, Trench-volcano gap along the Alaskan-Aleutian arc: facts, and speculations on the role of terrigenous sediments. In M. **Talwani** and W. **Pitman** (Ed.), Island Arcs, Deep Sea Trenches and Back Arc Basins, Maurice Ewing Series I. Am. **Geophys.** Union, 243-258, 1977.
- Kanamori**, H. The energy release in great earthquakes. J. Geophys. Res., 82, 2981-2987, 1977.
- Kienle**, J., S. E. Swanson, and H. Pulpan, **Magmatism** and subduction in the Eastern Aleutian Arc, In, D. **Shimuzuru** and I. **Yokoyama (eds.)** Arc Volcanism: Physics and Tectonics, Terra Scient. Publ. Co., (TERRAPUB), Tokyo, 191-224, 1983.

- Lahr, J. C., Hypoellipse/multics:** A computer program for determining **local** earthquake **hypocentral** parameters, magnitude and first motion patterns, U.S. Geol. Survey, Open File Report, 80-59, April 1980.
- Lahr, J. C., and G. **Plafker**, Holocene Pacific-North American Plate Interaction in Southern Alaska: Implications for the **Yakataga** Seismic Gap, Geology, 8, 483-486, 1980.
- Magoon, L. B., A. H. Bouma, M. A. Fisher, M. A. Hampton, E. W. Scott, and C. L. Wilson**, Resource Report for Proposed OCS Sale No. 60, Lower Cook **Inlet-Shelikof** Strait, Alaska, U.S. Geol. Survey, Open-File Report 79-600, 38 pp., 1979.
- Matumoto, T. and R. Page**, **Microaftershocks** following the Alaska earthquake of 28 March 1964: determination of hypocenters and **crustal** velocities in the **Kenai** Peninsula-Prince **William** Sound Area. In The Prince William Sound, Alaska Earthquake of 1964 and Aftershocks, **2B.**, U. S. Government Printing Office, 1969.
- McCann, W. R., S. P. **Nishenko**, L. R. Sykes, and J. Krause, Seismic gaps and plate tectonics: seismic potential for major boundaries, Pure Appl. Geophys., 117, 1082-1147, 1979,
- Pulpan, H., and C. **Frohlich**, Joint hypocenter determination of **teleseismically** recorded earthquakes on the Kodiak Shelf, Alaska, OCSEAP Annual Reports of Principal Investigators, RU 597, 1982.
- Pulpan, H. and C. **Frohlich**, Earthquake relocation by the joint hypocenter determination method in Kodiak Island and Lower Cook Inlet areas of Alaska (submitted for publication).
- Pulpan, H. and J. **Kienle**, Western Gulf of Alaska Seismic Risk, **Proc. Offshore Tech. Conf.**, April 30-May 3, 1979, Houston, Texas, 1, 2209-2219, 1979.

- Reyners, M.** and **K. S. Coles,** Fine Structure of the dipping seismic zone and subduction mechanics in the **Shumagin** Island, Alaska. J. Geophys. Res., **87**, 356-366, 1982.
- Richter, C. F., Elementary Seismology, **W. H. Freeman and Co.**, San Francisco, CA, 768pp., 1958.
- Romanowicz, B.**, Depth resolution of earthquakes in central Asia by moment tensor inversion of long period Rayleigh waves, J. Geophys. Res., **86**, 5963-5984, 1981.
- Samowitz, I. R.** and **D. W. Forsyth,** Double seismic zone beneath the **Mariana** Island arc, J. Geophys. Res., **86**, 7013-7021, 1981.
- Stoiber, R. E.** and **M. J. Carr,** Quaternary volcanic and tectonic segmentation of Central America. Bull. Volcanologique, **73**, 304-325, 1973.
- Sykes, L. R., Aftershock zones of great earthquakes, **seismicity** gaps, and earthquake prediction for Alaska and the Aleutians, J. Geophys Res., **76**, 8021-8041, 1971.
- Sykes, L. R., J. B. Kissinger, L. House, J. Davies, and K. H. Jacob, Rupture zones and repeat times of great earthquakes along the **Alaska-Aleution** arc, In, Earthquake Prediction, Maurice Ewing Series, **4**, Amer. Geophys. Union, 1981.
- Tobin, D. G. and L. R. Sykes, Relationship of hypocenters of earthquakes to the geology of Alaska, J. Geophys. Res., **71**, 1659-1669, 1966.
- Van Wormer, J. D., J. Davies and L. Gedney, **Seismicity** and plate tectonics in south central Alaska, Bull. Seismol. Soc. Amer., **64**, 1467-1475, 1974.
- Veith, K. F.**, The relationship of island arc **seismicity** to plate tectonics, Ph.D. thesis, Southern Methodist University, 1974.

Woodward-Clyde Consultants, Offshore Alaska Seismic Exposure Study.

Report prepared for Alaska Subarctic Operators Committee, 6 volumes,
1978.

Woodward-Clyde Consultants, Development and Initial Application of Software
for Seismic Exposure Study, Report to NOAA, 2 volumes, **1982**.

APPENDIX

EPI CENTER PLOTS 1978-1982

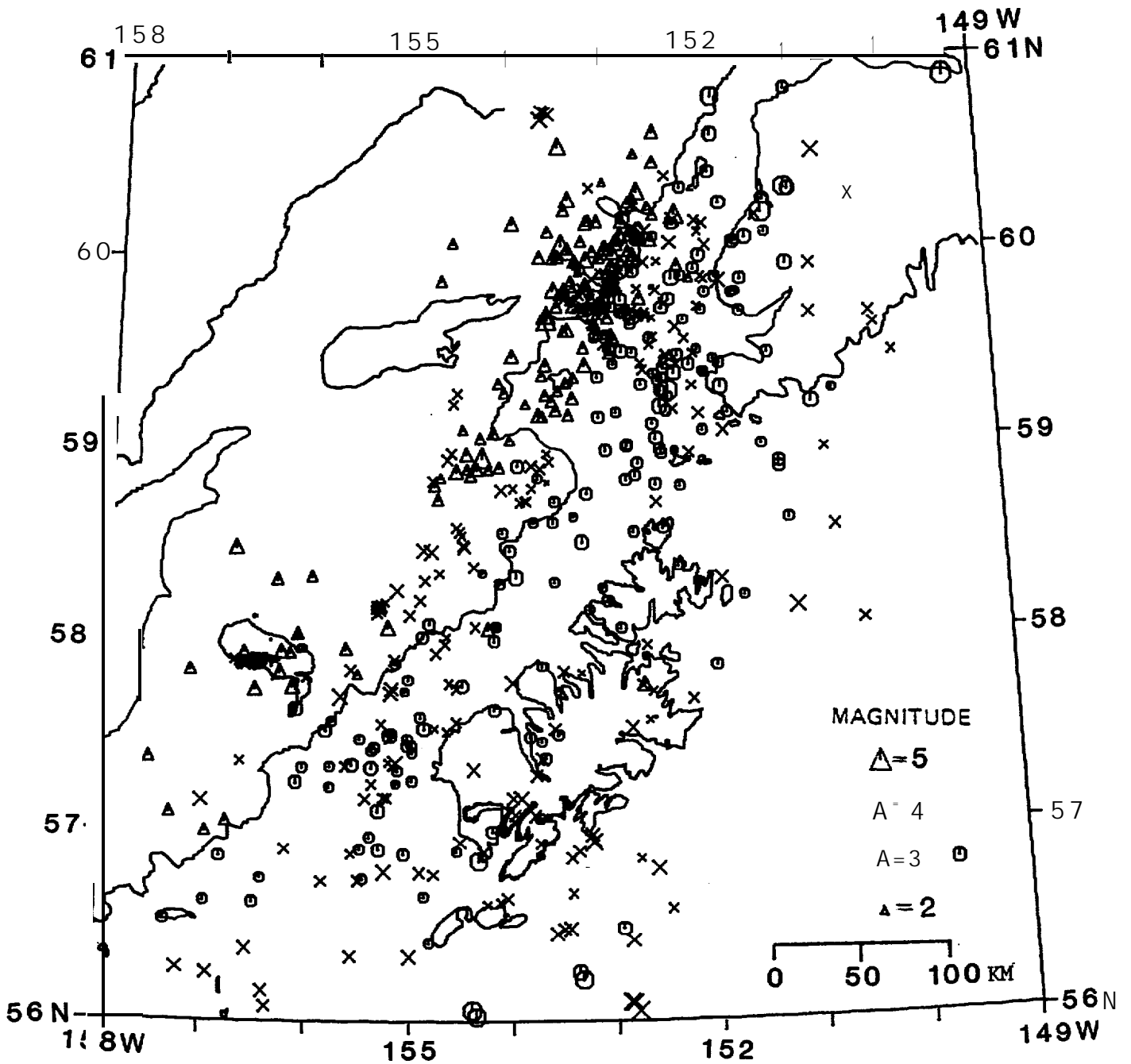


Figure A1: Epicenters of all earthquakes located during January-March, 1978. Symbols indicate depth range of events: crosses 0-35 km, circles 36 to 100 km, and triangles deeper than 100 km.

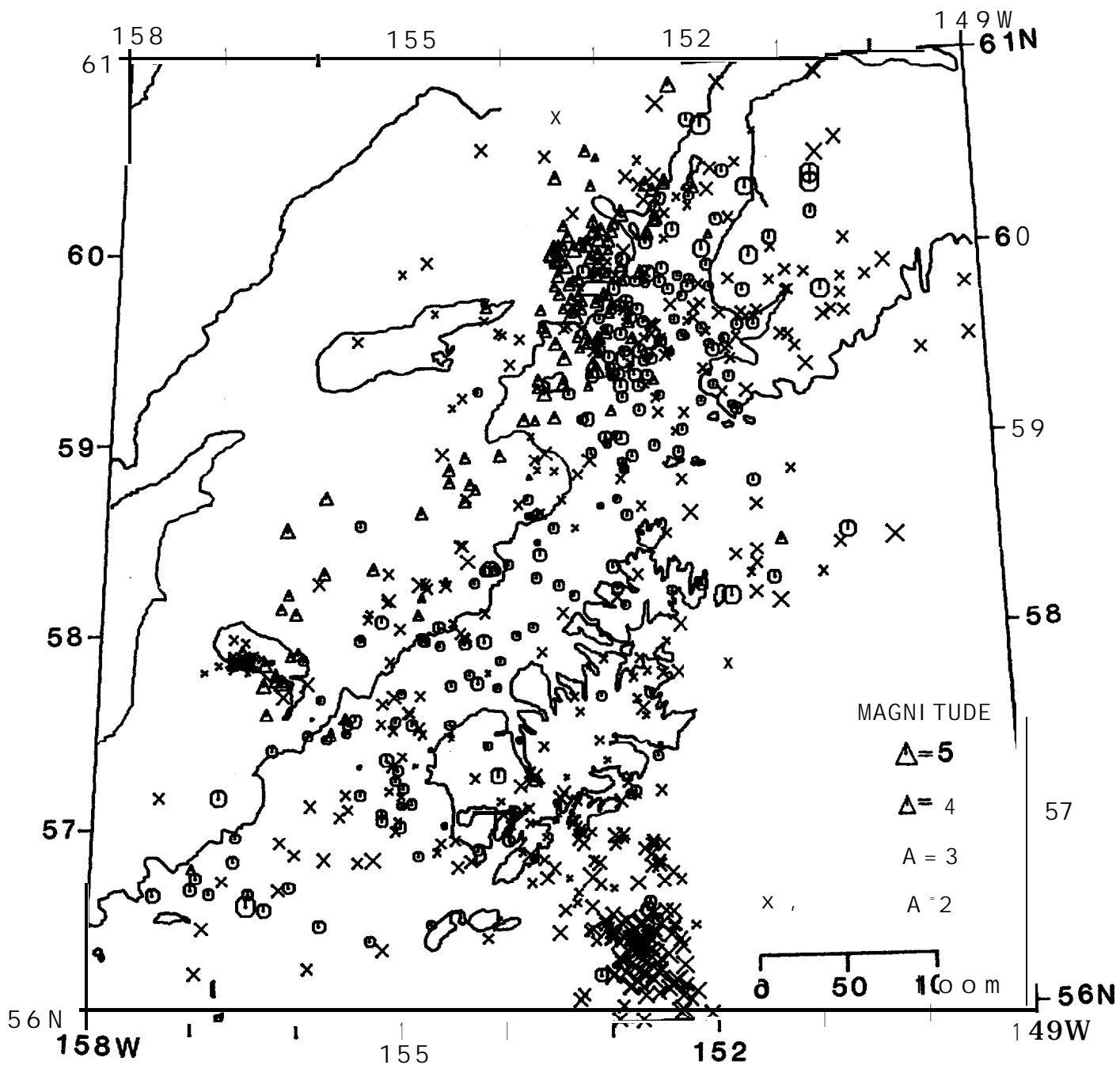


Figure AZ: Epicenters of all 11 earthquakes located during April 1 - June, 1978. Symbols as in Figure AI.

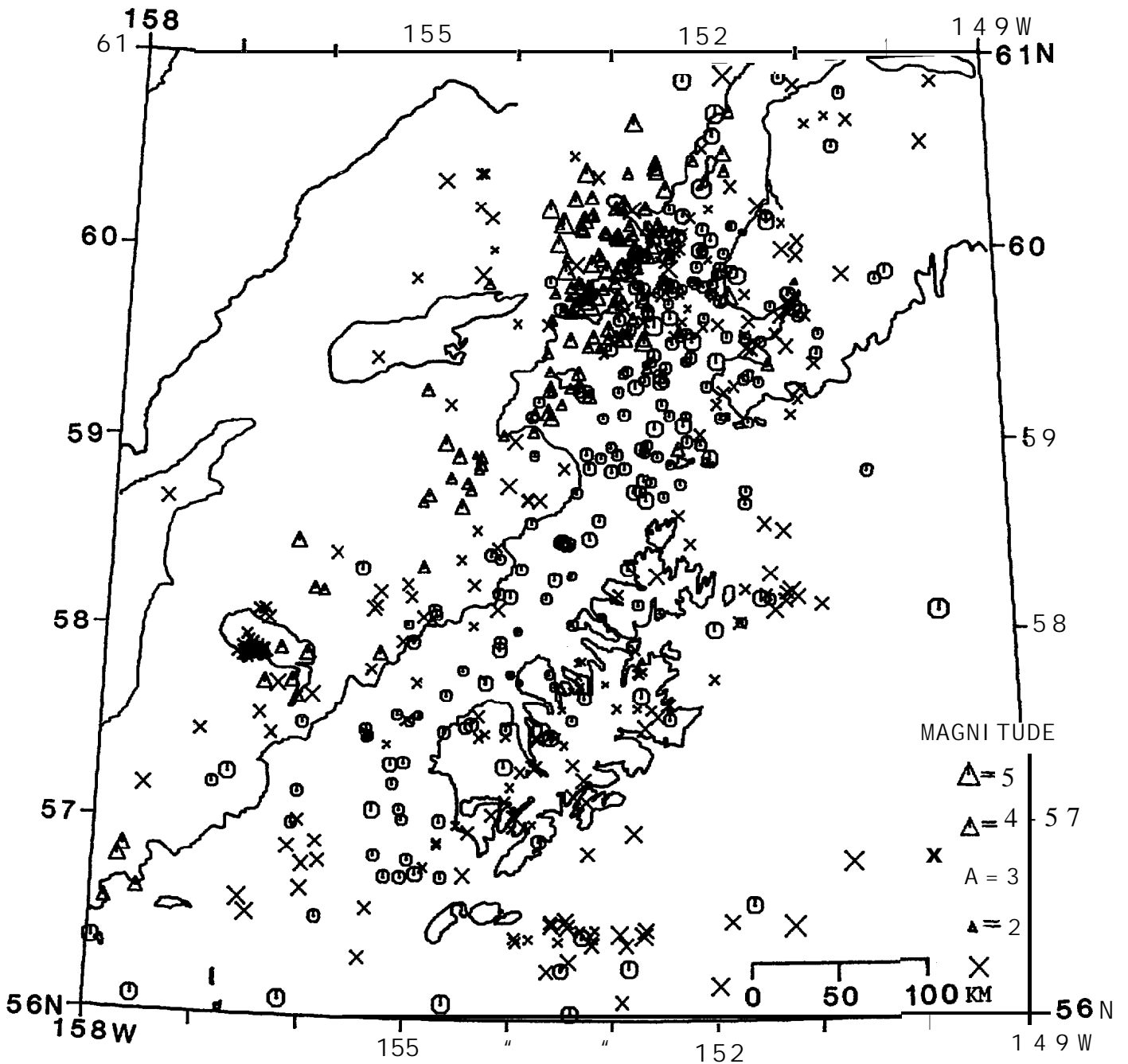


Figure A3: Epicenters of all earthquakes located during July-September, 1978. Symbols as in Figure A1.

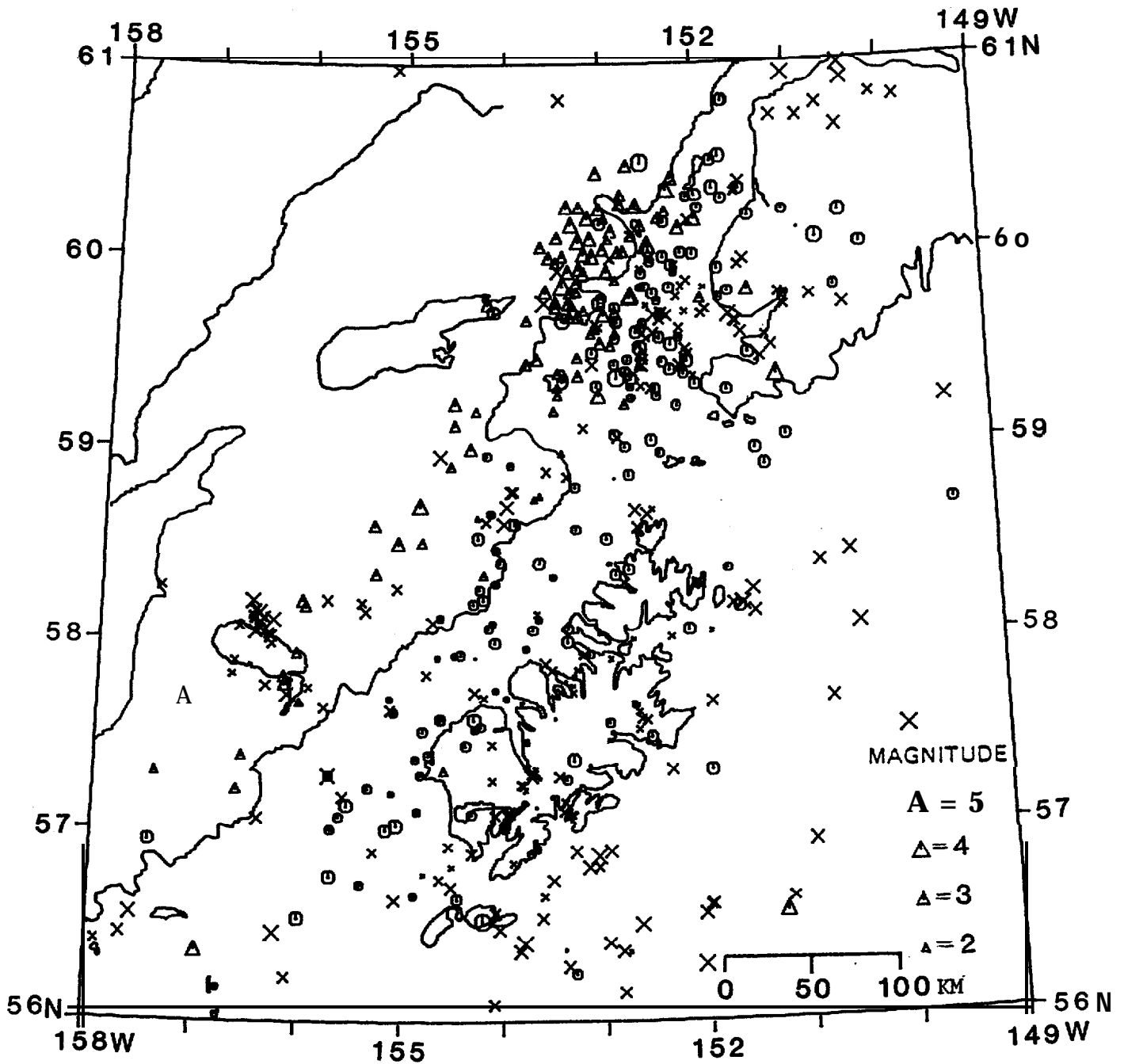


Figure A4: Epicenters of all earthquakes located during October-December, 1978. Symbols as in Figure A1.

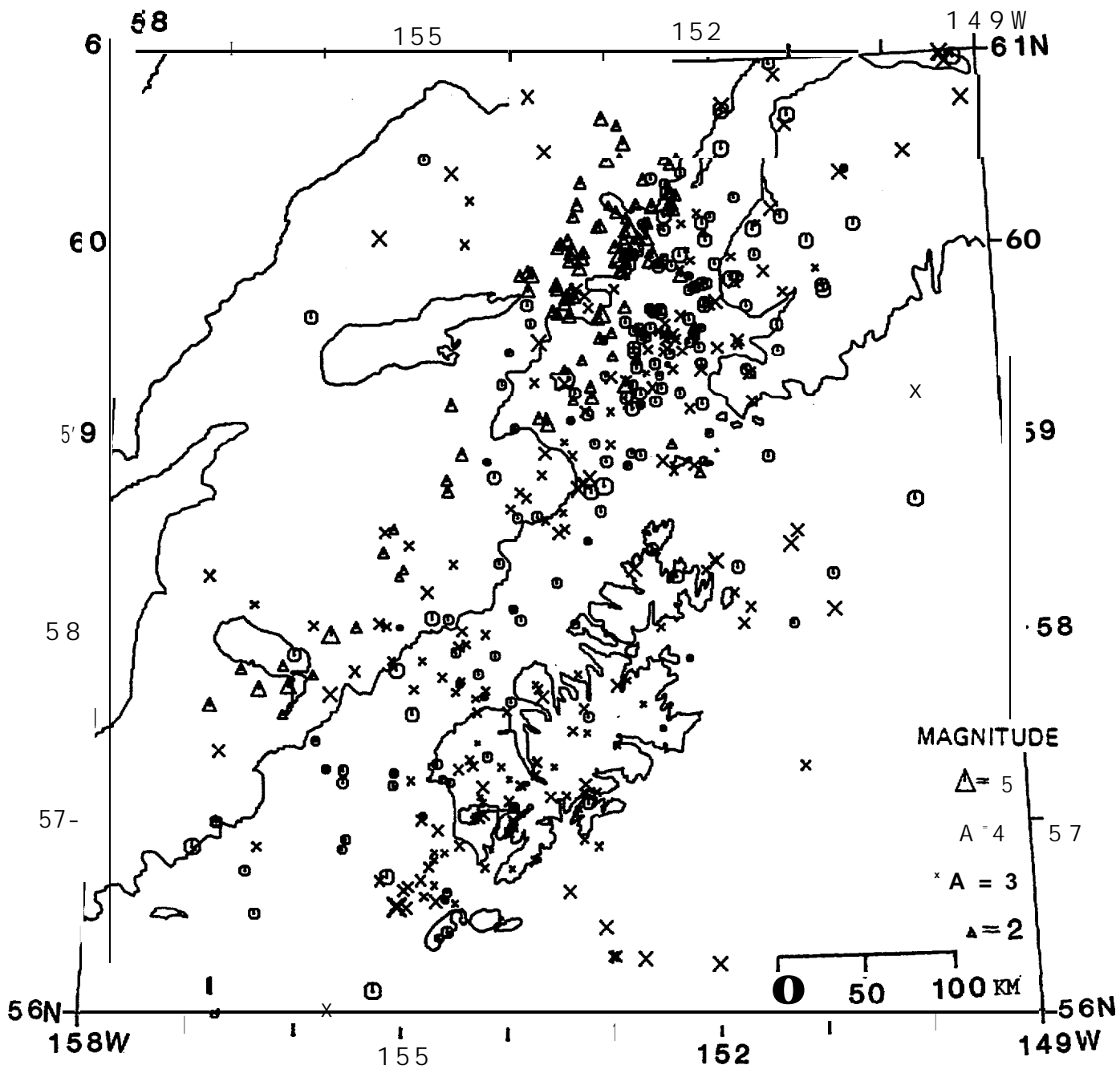


Figure A5: Epicenters of all earthquakes located during 1979. Symbols as in Figure A1.

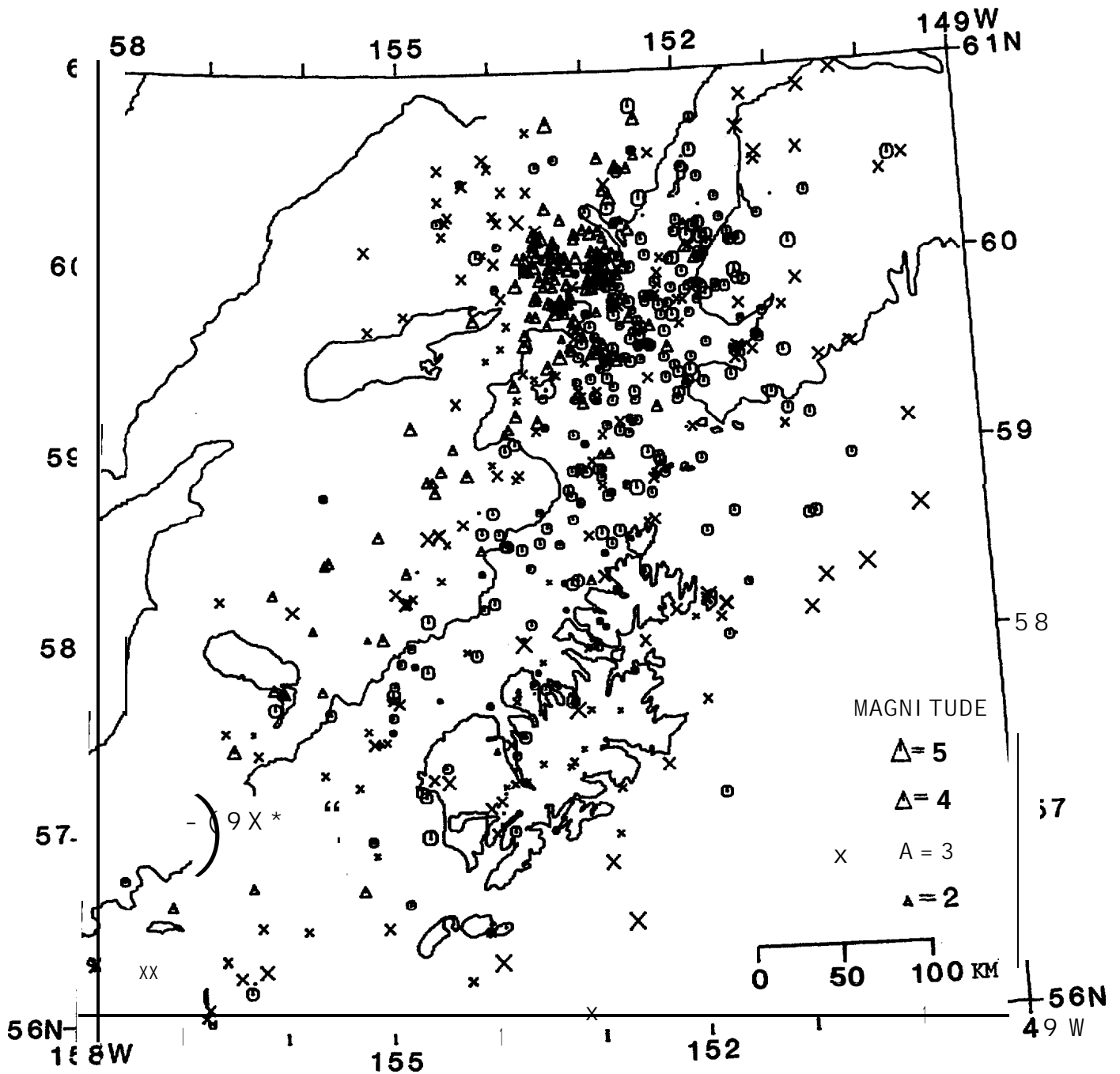


Figure A6: Epicenters of all earthquakes located during January-June, 1980. Symbols as in Figure A1.

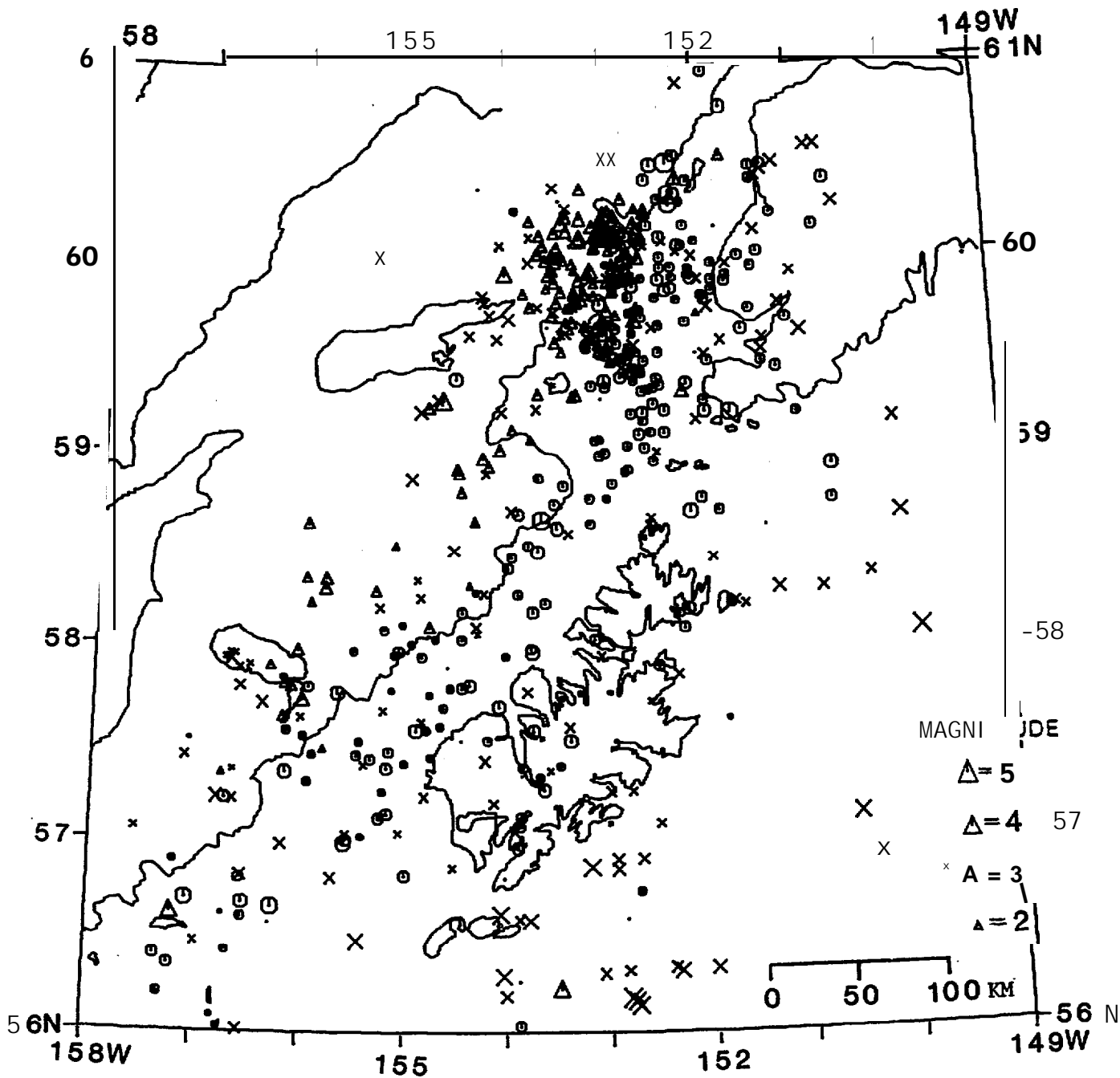


Figure A7: Epicenters of all earthquakes located during July-December, 1980. Symbols as in Figure A1.

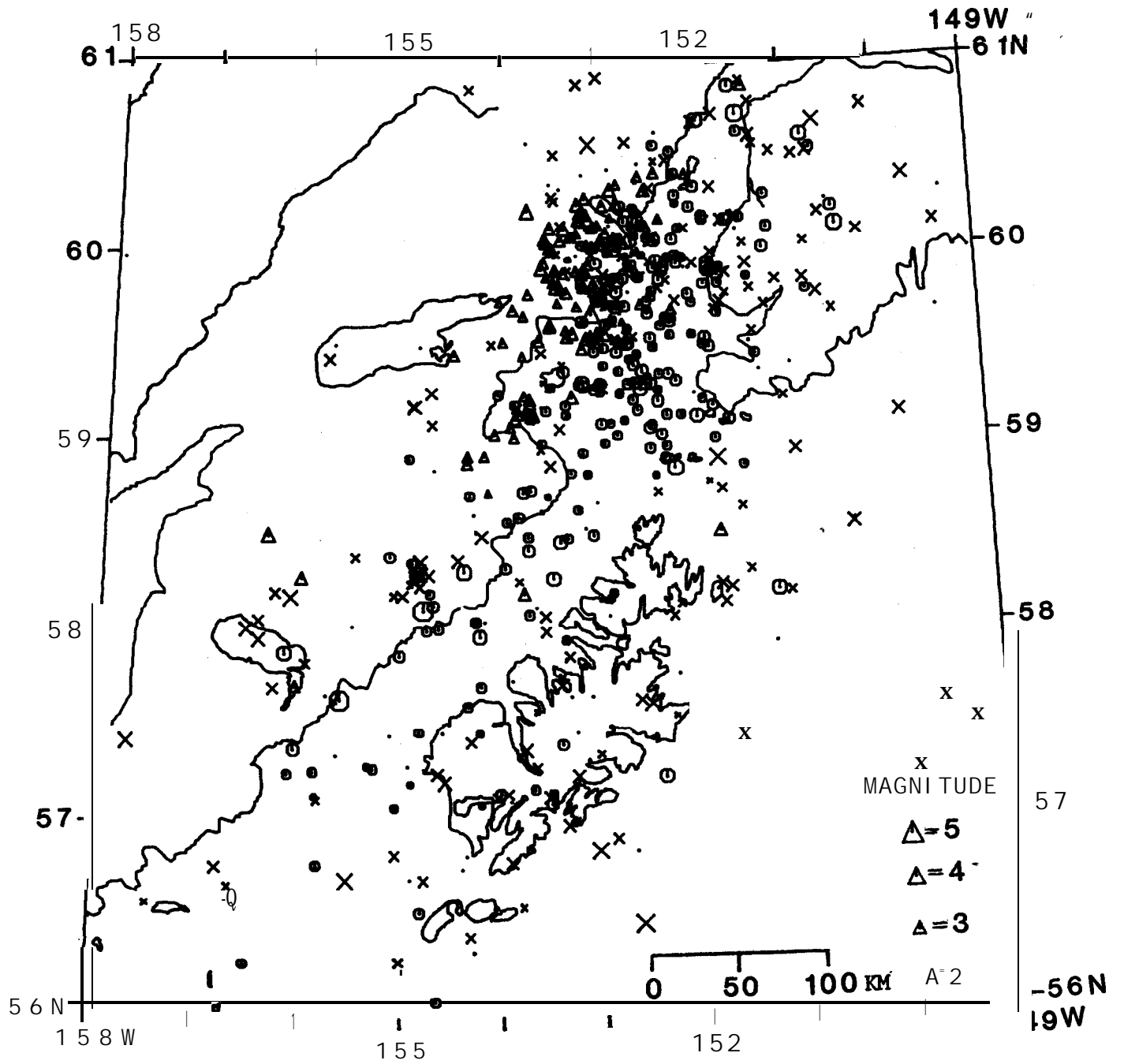


Figure A8: Epicenters of all earthquakes lotted during January-June, 1981. Symbols as in Figure A1.

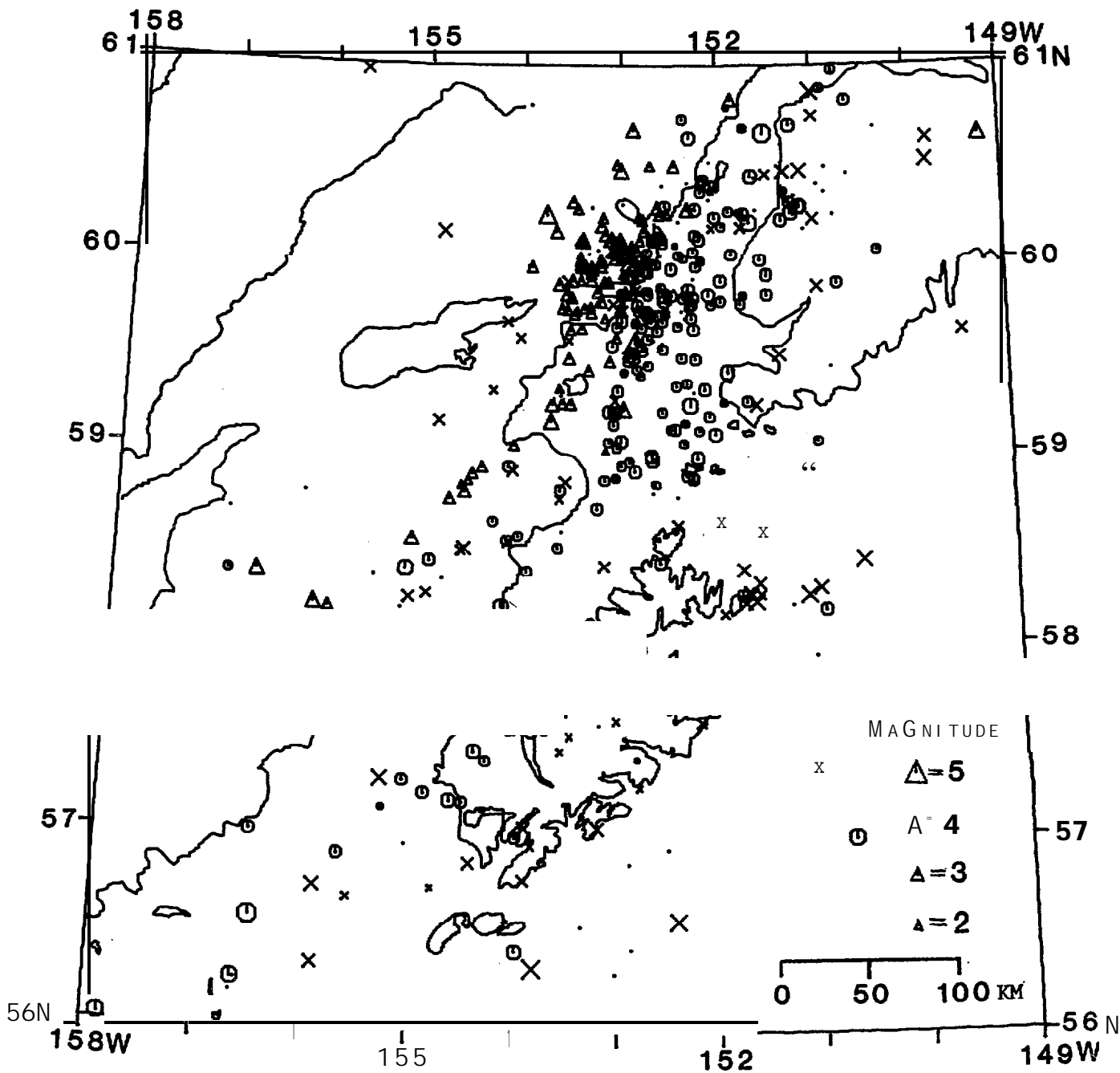


Figure A9: Epicenters of all earthquakes located during July-December, 1981. Symbols as in Figure A1.

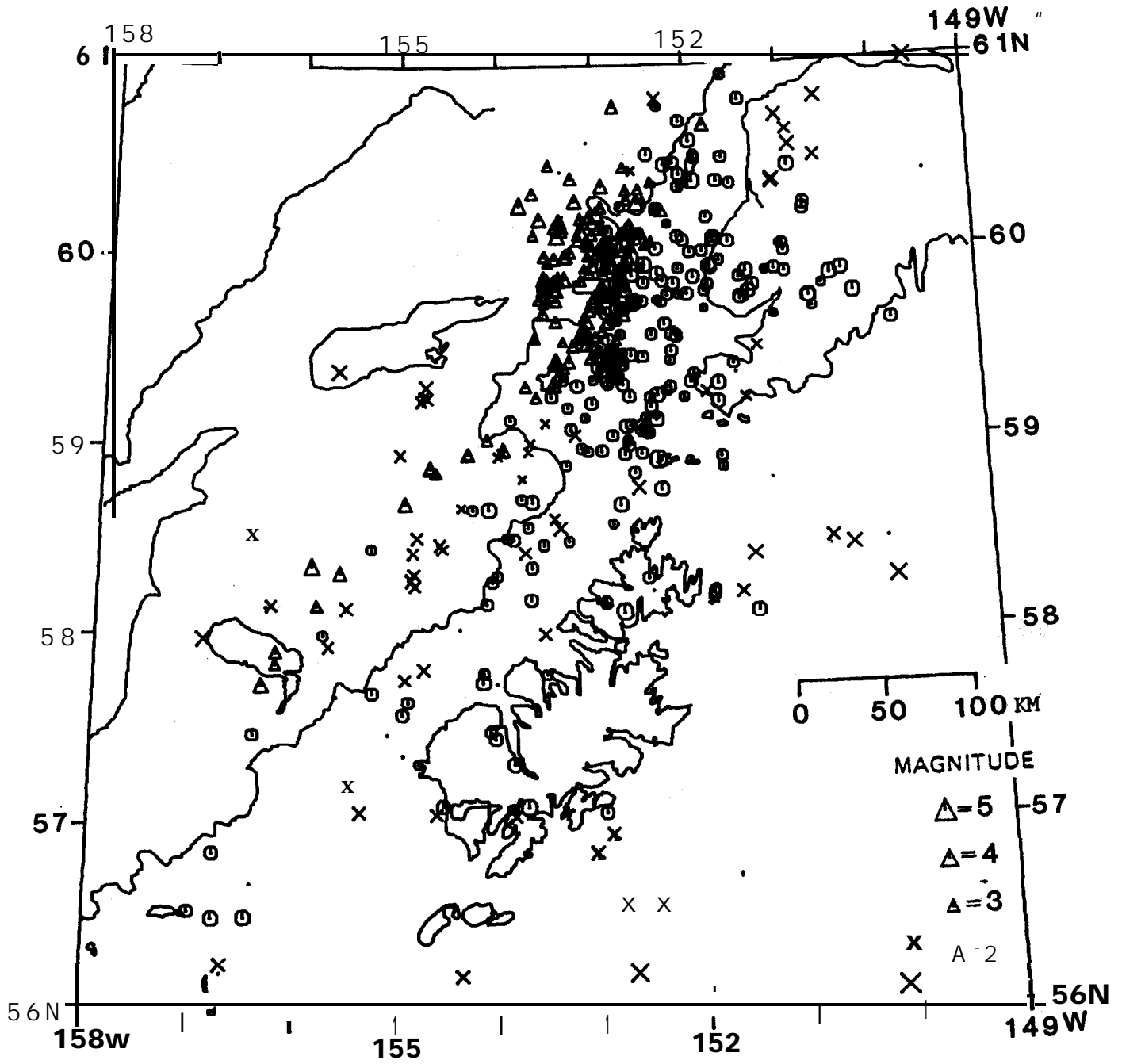


Figure A10: Epicenters of all earthquakes located during 1982. Symbols as in Figure A1.